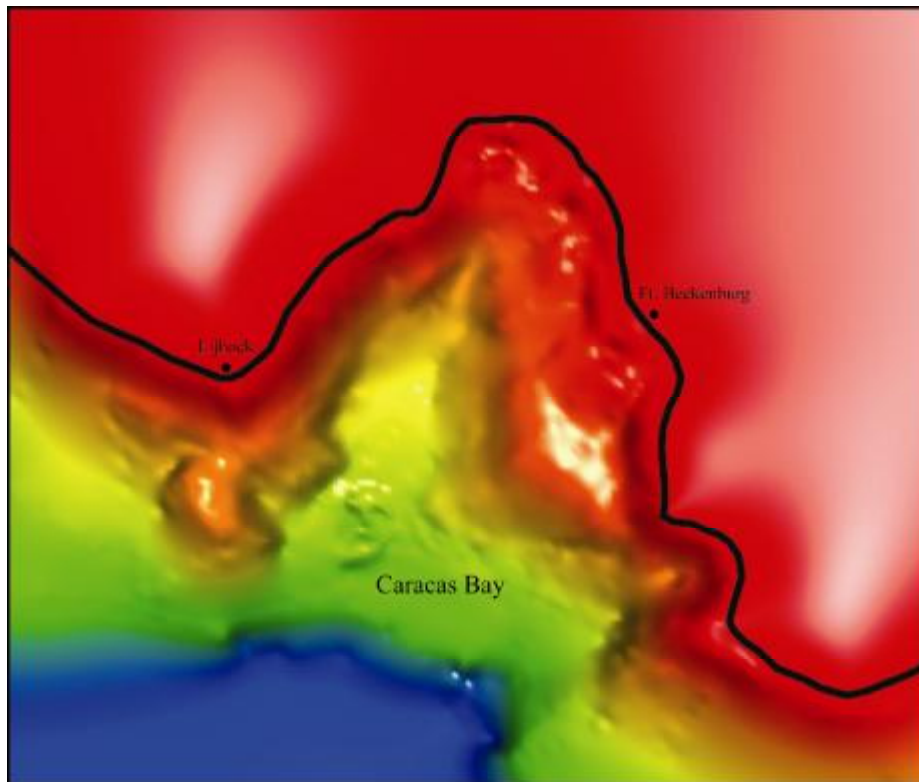


# **Assessing Slope Stability at Seroe Mansinga and Caracas Bay, Curacao**

**Final Report for APNA, Willemstadt, Curacao**



**Prepared By:  
Dr. Matthew J. Hornbach  
Dr. Paul Mann  
Dr. Sabine Wolf  
Mr. William King  
Ms. Rebecca Boon**

**The University of Texas at Austin  
Jackson School of Geosciences  
Tuesday, February 5th, 2008**

## Preface

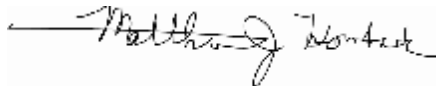
The following final report to the project sponsors consists of geological, core and technical analysis of Caracas Bay area, Curacao, in order to assess the site stability of the APNA real estate development located along the elevated hill (Seroe Mansinga) that forms the western edge of Caracas Bay. Over the past six months, our team of geoscientists completed 10 days of field studies and have spent several months analyzing seismic data, geological observations and maps, and sediment cores from bays surrounding Caracas Bay with the goals of characterizing: 1) geologic setting of Seroe Mansinga and Caracas Bay, 2) slide/erosion history of Caracas Bay as first noted in the publication by DeBuissonje and Zonnenfeld (1976), 3) quantification of slide trigger frequency based on coring results, seismic analysis, published studies, and occurrence of large earthquakes in the region, 4) quantification of probability of future sliding and large-scale erosion of the eastern edge of Seroe Mansinga adjacent to Caracas Bay, and 5) suggestions for how future work would build on the geological and probabilistic analysis presented here to better assess the site stability of the area.

We are pleased to report that this final, six month analysis has produced tangible results that draw valuable first-order conclusions with clear implications for the stability of Seroe Mansinga and Caracas Bay. We presented an initial progress report on the project one month after the field work was completed on September 26, 2007, as outlined in the original proposal to APNA.

This final report focuses on merging geological interpretations of the land areas surrounding the bay and marine seismic results (100% of the marine seismic data and core results have now been fully processed and incorporated into this report) with structural analysis and statistical methods. Integration of these observations further develops the earlier observations of DeBuissonje and Zonnenfeld (1976) and places new constraints on the age of the main slide creating Caracas Bay, rates of mass wasting along the cliff defining the western edge of the bay, areas at risk of slumping along the eastern edge of Seroe Mansinga, and the probability of future sliding or faulting at the site.

Our technical analysis points out a few additional tasks that would strongly compliment this study and could be accomplished by engineers. We have been in communication with Dr. Bob Gilbert of the University of Texas at Austin Department of Engineering concerning future engineering studies related to this project. If it is warranted, we encourage the sponsors to contact Dr. Gilbert with regards to a follow-up study. We consider this report as final. We appreciate the invitation and support of APNA for us to work on this interesting and important study in Curacao.

Sincerely,



Dr. Matthew J. Hornbach et al.  
The University of Texas at Austin  
Jackson School of Geosciences  
Institute for Geophysics

## **Introduction**

This report represents a final six month analysis of our geological findings and analysis at Caracas Bay and Seroe Mansinga. Specifically, this work consists of the following three sections: (1) a report describing the land and sea geological/seismic results and analysis, (2) a report on coring results and analysis, and (3) a statistical analysis of structural failure at the site. We make 3 recommendations regarding possible future study at the end of this report.

## **Final report: Part I** **Land- and sea-based geological/seismic observations and analysis**

### **A. Geographic and geological setting of Caracas Bay**

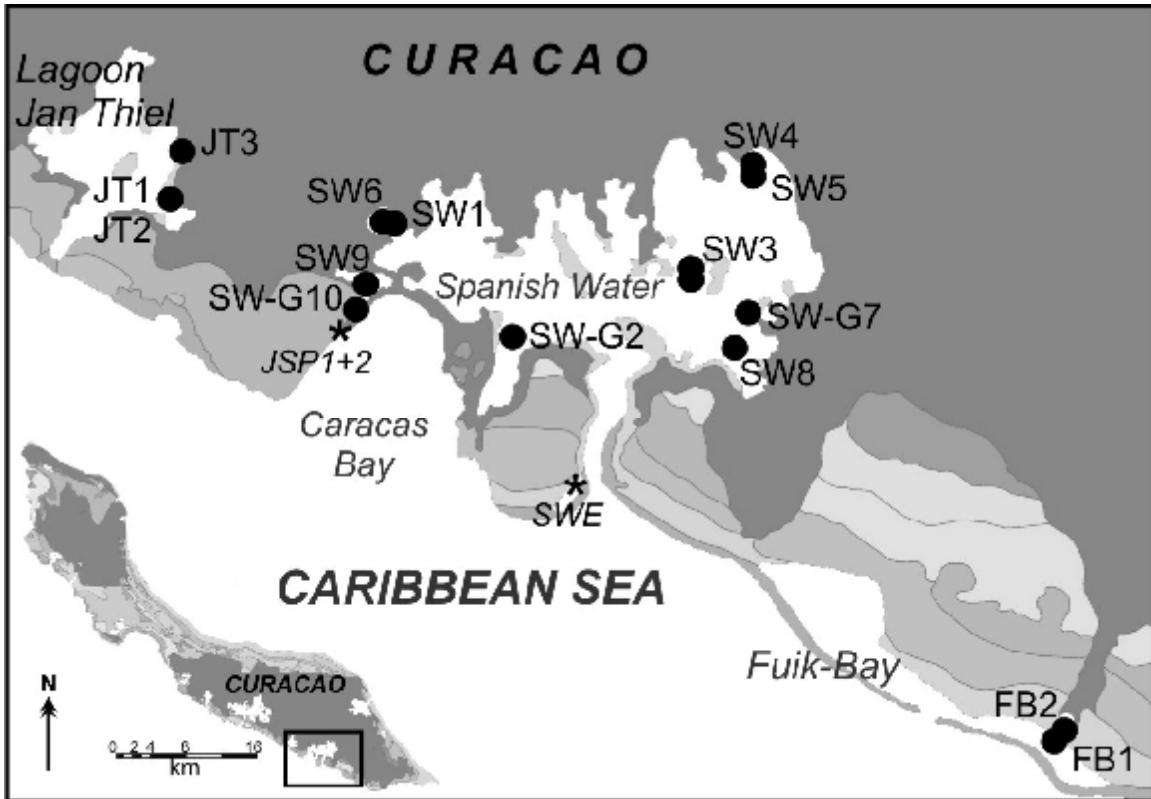
Curacao (12°2'-12°23' N and 68°44'-69°10' W) is the largest of the three Leeward ABC Islands (Aruba, Bonaire, Curacao) of the Netherlands Antilles, and is situated in the Southern Caribbean Sea about 70 km from the coast of Venezuela. Curacao Island is at most 61 km long and 14 km wide with a total area of 444 km<sup>2</sup>. It is a densely populated island with 140,000 inhabitants who represent ca ¾ of the entire population of the Netherlands Antilles.

Curacao is geologically characterized by two main rock types, Cretaceous basalt and Tertiary limestone (Fouke, 1994; Beers et al., 1997) (Fig. 1-1). The basalts (diabase) represent the oldest unit of the island and constitute a succession of up to 5000 m thick lava formation which was extruded submarine between 100 and 85 million years ago (Middle – Late Cretaceous). The limestone is of Miocene, Pliocene and Quaternary age, and represent fossil reef and fore-reef deposits. The limestone units form the characteristic seaward-dipping limestone hogbacks on the leeward side of the island. Results from studies of terrace deposition of windward and leeward flanks of the island yield low uplift rates that range from 0.02 to 0.08m/1000 years, with an estimated average of 0.05m/1000 years (Fouke, 1994). The tectonic uplift of the Curacao horst was initiated in the Middle Miocene and continued into the Pleistocene and Holocene.

As in other areas, the strong contrast between potentially clay-rich basalt and seaward dipping limestone produces a setting favorable for large slides (eg. Fryman et al., 2007). The uppermost parts of the younger Pleistocene reefs are characterized by terrestrial karstification and bio-erosive rock pool formation, and are less resistant than

the lower reef sections which are covered by modern bio-constructions. This in combination with the recurrence of waves makes the coastlines of Curacao

**Figure 1-1:** Schematic geological map of Curacao Island. Dark grey fields: Curacao Lava Formation (diabase; Upper Cretaceous); medium and light grey fields: Coral limestone (Quaternary) and Midden Curacao Formation (Tertiary conglomerates, sandstones). Black circles mark coring locations; black stars indicate coral rubble sample location. All units dip about 10 degrees to the southwest. Note the large gap in the coastal units at Caracas Bay that have apparently slid into deeper water.



vulnerable to failure along the cliff. One catastrophic landslide occurred most likely in Holocene times in the Caracas Bay in the southeastern part of the Island, when a 45-to-250 m thick limestone block covering an area of 1 km<sup>2</sup> broke free, plunged into the ocean, plowing a 1 km wide, 50 m deep channel into the ocean floor as it accelerated into the abyss (De Buissonje and Zonneveld, 1976). The slide(s) left house-size boulders strewn across the beach, displaced thousands of cubic meters of sediment from the seafloor, and, according to modeling results, likely spawned tsunami that may have exceeded 5 m in height.

Curacao has a steppe climate, which is characteristic for the area along the northern coast of South America. The strong trade wind has an annual average speed of 6.9 m/s (at 10m height) and an average north-easterly direction (Meteorological Service of the Netherlands Antilles). The average temperature is 27.6°C with only small monthly variation up to 1.4°C and small differences throughout the year (4-5°C). Curacao lies outside the Atlantic hurricane belt, but can still occasionally be impacted by hurricanes. The typical Hurricane season is between June and November with an annual frequency between 1 and 21 events.

During the time period 1605 – 2000 in total 14 hurricanes and 19 tropical storms with maximum wind velocities between 100 – 120 mph near the center passed the ABC islands within the 100 nm zone. Most of these hurricanes track from east to west and therefore strongly impact the eastern and northern shores of the ABC Islands (i.e. Hurricane “Ivan” in 2004). Extremely rare exceptions to these paths and impact patterns are given by west to east tracking storms such as Hurricane “Lenny” (1999) and a Hurricane in 1877; those events mainly affected the normally sheltered western and southern coastlines of the ABC Islands (Scheffers and Scheffers, 2006).

The shoreline of the island is interrupted by several hand-shaped inland bays and tiny pocket beaches, so-called Bocas, which formed during Holocene sea-level rise. The complex dendritic shape and arms of Willemstad harbor and Spanish Water are both examples of flooded river valleys that formed during the Holocene sea level rise.

## **B. Results of geologic observations and mapping**

**i. Introduction.** Three days were devoted in August, 2007, to examining the onland area surrounding the bay that was previously described by DeBuissonje and Zonnenfeld (1976). We summarize the results of our geologic study with their previous mapping and our new geologic and bathymetric observations on the map in Figure 1, and figure 1-1. Air photos were georeferenced in GIS, merged with offshore bathymetry, and used as basemaps to better show cultural and geologic features. We chose an older, 1960’s era photo as the basemap for Seroe Mansinga because it reveals the trend of bedding planes across the upper surface of the hill; these bedding planes are now obscured by house and road building.

All maps for this project were prepared in ArcGIS v. 9.2 to insure that features were accurately georeferenced. We have compiled as many photos and topographic maps as available through government agencies and included older photographs that appeared in previous publications (these photos were not available through agencies in Curacao). ArcGIS allows all of these materials be to georeferenced in an exact geographic context.

**ii. Cliff face along the eastern edge of Seroe Mansinga.** The west to east bathymetric asymmetry of Caracas Bay with a much deeper western area (100-150 m) adjacent to the 10-50 m high cliff and the shallower (50-90 m) eastern part of the bay (Fig. 1) is consistent with the previous interpretation by DeBuissonje and Zonnenfeld (1976) that the western face forms the breakaway scarp for a large seaward-moving slide dated by them as 10,000-30,000 years before the present.

The geology of the cliff face consists of two different geologic units that are both classified as the Tertiary Seroe Domi Formation: the area to the north in the cliff consists of a poorly bedded massive limestone unit that is subject to mass wasting along the cliff edge, particularly in the area indicated on Figure 1 (and Fig. 4). A more thinly bedded and erosionally resistant limestone unit forms the southern part of the cliff and is less subject to slumping along the steep cliff that forms the eastern limit of Seroe Mansinga (Fig. 2).

**iii. Geologic structure of Seroe Mansinga.** Cretaceous basalt underlies the Seroe Mansinga and dips gently seaward to the southwest based on previous regional mapping by DeBuissonje and our own observations (Fig. 1). We did not observe any basaltic outcrops along the southern edge of the small lagoon that forms the northern edge of Seroe Mansinga as previously reported by DeBuissonje and Zonnenfeld (1976). It is likely that these outcrops were covered during dumping of material related to the clearing of house sites on the north slope of Seroe Mansinga. We infer that this basalt dips about 10 degrees southward beneath the Seroe Mansinga based on our measured dips of basal dolomitic limestone adjacent to the lagoon and farther to the north in the development area, which is also consistent with previous studies (Figure 1). We did not directly observe the basalt-limestone contact in any outcrop we visited and therefore cannot make

any conclusions about whether this contact is a depositional contact or has been affected by sliding of the Seroe Mansinga limestone off of the underlying basalt.

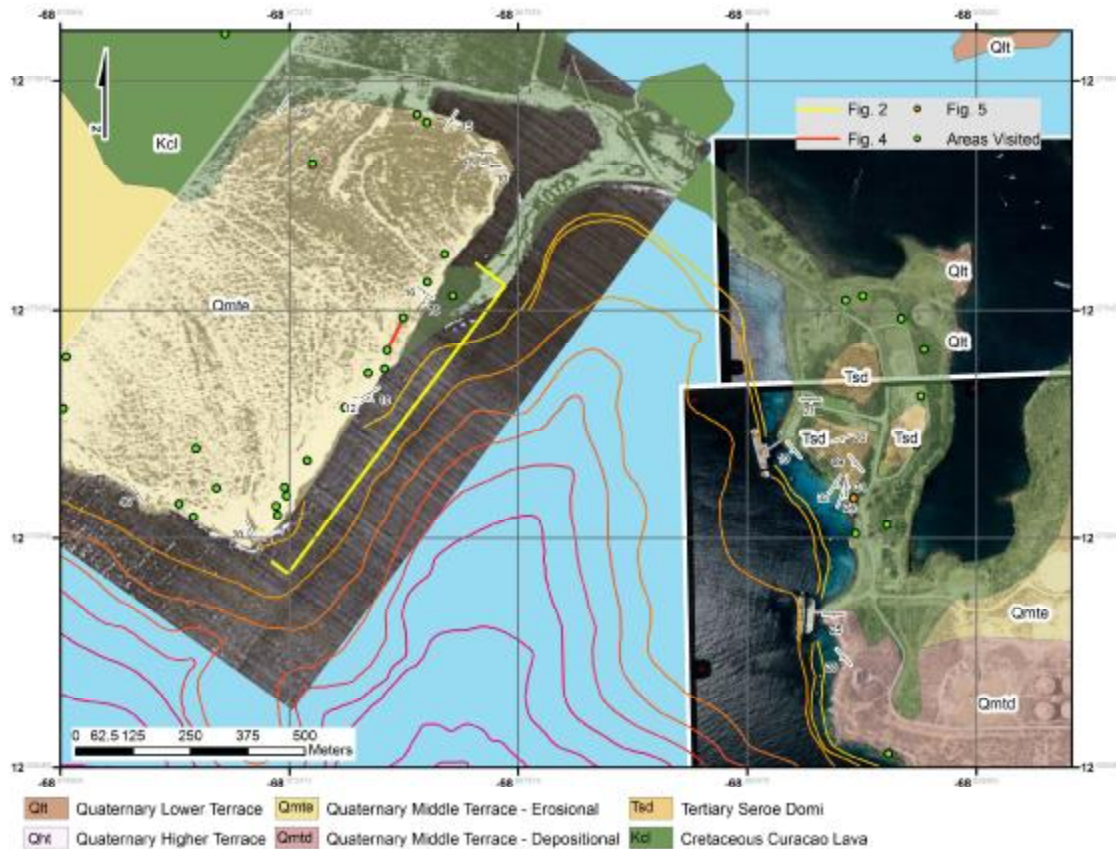


**Figure 1.** Map integrating new bathymetry from Caracas Bay with surrounding geologic units taken from DeBuissonje and Zonneveld (1976). Western Air photo is a 1960's image scanned from DeBuissonje and Zonneveld (1976). Eastern Air photo was taken from the Curacao-DOW survey in 1998. Strike and dip measurements were made by Mann and King for this project. Green dots show all outcrops visited by us for this study and located with GPS. Yellow bar shows extent of photo montage in Figure 2 of the cliff at the western edge of Caracas bay. Comparison of position of cliff edge over the past century is shown on Figure 3. Two green dots connected by red line at the top of the scarp is the location of open fissures at the top of the scarp as shown in the photo in Figure 4.



**Figure 2.** Photomontage of cliff face along western side of Caracas Bay (southwest is to the left with the small lighthouse marking the south coast of Seroe Mansinga; northeast is to the right). More massive limestone to the northeast along the highest part of Seroe Mansinga is more subject to mass wasting of



large boulders than the thinner bedded and more erosionally resistant limestone in the lower elevations to the southwest. Faults with minor (meter-or-less) offsets can be seen along the southern side of the cliff.

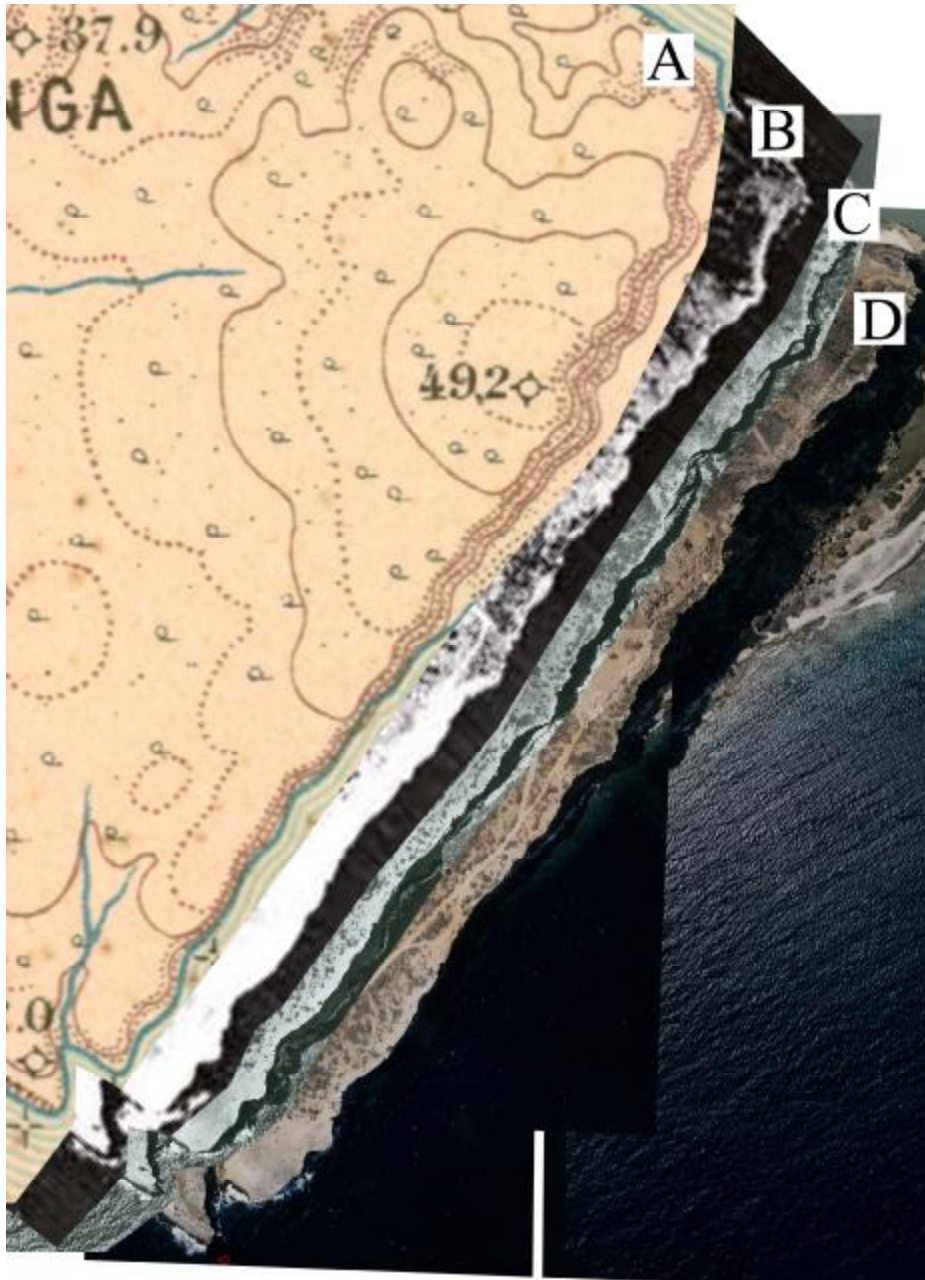


**Figure 3.** Comparison of the position of the cliff face along the western edge of Caracas Bay at four times over the past century: 1906, sometime in the 1960's, 1989, and 1998. The positions of the coastlines at the four time are staggered to show similarities and are not in a geographic context. Note that the the position and overall shape of the cliff face has remained relatively unchanged since the first topographic survey of Curacao by Werbata in 1906. Mass wasting of the cliff face is a potential problem especially in the area marked by the red line on the map in Figure 1 because of the fractured and cavernous, massive



*limestone as shown in Figure 2 and the existence of large open fissures aligned parallel to the cliff face as shown in Figure 3.*

*A = Werbata (1906)*

*B = taken from DeBuissonje and Zonneveld (1976) (original air photo taken during the 1960's)*

*C = KLM AeroCarto (1989)*

*D = Curacao - DOW (1998)*



**Figure 4.** *Photo taken at the top of the cliff face looking north along the western edge of Caracas Bay showing large fissure that has formed parallel and about 5 meters landward of the vertical cliff face. Note that the road along the eastern edge of the APNA development is visible to left of the photo. The fissure runs from the viewer to the person in middle distance and extends as an open crack several meters downward into the fractured and cavernous massive limestone beneath the surface. The fissure remains open despite efforts to fill in the fissure with soil, rocks, scrap metal, and other debris. Large boulders at the base of the cliff in this area attest to previous, sudden mass wasting events of limestone boulders along the cliff face. Based on the maps shown in Figure 3, the locations of these sudden mass wasting events are not detectable from 1906 to 1998.*



**Figure 5.** Photo looking northward of a large limestone boulder of the Seroe Domi Formation directly overlying Cretaceous basalt near Fort Beekenburg on the Caracas Bay peninsula east of Caracas Bay. The limestone block dips gently about 10 degrees towards the viewer. Following DeBuissonje and Zonneveld (1976) we interpret this block and surrounding limestone blocks of comparable or larger size as slide blocks along the top of a gently seaward upper surface of basalt. Dips in the limestone strata in the distance near Fort Beekenburg are highly variable (note dip in that area is more to the right or to the east – cf. map in Figure xx) and suggest that a larger limestone block may have slid along the top of the basalt layer in the Fort Beekenburg area.

A large eastward-plunging syncline or fold structure is present in the northeastern part of Seroe Mansinga as seen from the trend of bedding planes across the erosional upper surface of the hill. These bedding planes are now obscured by housing and roads built in this area. The tectonic origin of this fold is not clear since no comparable structure is found in any other area of the Seroe Domi Formation of Curacao (DeBuissonje and Zonnenfeld (1976). The uniqueness of the syncline and its location adjacent to the Caracas Bay slide suggests the possibility that it formed as a result of the same sliding event that formed Caracas Bay. The force required to move the limestone unit (necessary to form such a syncline) is analyzed in section III.

According to the classification scheme of DeBuissonje and Zonnenfeld (1976), the upper surface of Seroe Mansinga correlates to the Quaternary Middle Terrace that is erosional in origin (Fig. 1). Several normal faults striking to the west-northwest are observed in the cliff face but are not seen as scarps in the upper surface of the hill (Fig.

2). These appear to be listric faults, with an average dip of ~30 degrees that reduce in angle with depth. The offset of these faults is on the order of meters or less, indicating relatively little slip has occurred along these faults in the past. Furthermore, these faults appear partly overlain by carbonate, suggesting limestone deposits may have formed after faulting. We have been unable to determine exact ages of the deposits overlaying the fault, however according regional maps, they are older Holocene, thereby suggesting these faults have not been active for ~10,000 years.

Younger Quaternary coral reef deposits are present along the southwestern, seaward edge of the hill. One area along this stretch of the coast exposes a more steeply dipping limestone unit that appears to be the substrate of the hill in this area and would correspond to the beds of the Seroe Domi Formation that make up the limbs of the large syncline more to the north (Fig. 1).

**iv. Mass wasting versus catastrophic failure of Seroe Mansinga.** Two similar but linked processes have affected Seroe Mansinga: present-day mass wasting of its steep eastern face along Caracas Bay and the catastrophic failure which was estimated by us to have occurred ~14,000 years ago. The large failure event, discussed at length later in this section and in part III of this report, produced the steep eastern face as a breakaway scarp to the landslide that was traced by DeBuissonje and Zonnenfeld (1976) to a depth of 700 meters in the offshore area.

Mass wasting is most prominent in the more massive limestone unit along the cliff face (Fig. 2). Important observations include the large car-sized boulders of the massive limestone present at the bottom of the cliff and the presence of fissure or open cracks parallel to the edge of the cliff in the area indicated on the map in Figure 1. These fissures extend several meters into the subsurface despite efforts by the developers to infill them with soil and other debris (Fig. 4). It is likely that these fissures will act as planes of weakness that will fail during future mass wasting events.

In order to better understand the rate of mass wasting and to evaluate its possible impact on housing on Seroe Mansinga, we placed four maps of the cliff face at the same scale in Figure 3. Map A is the first topographic map of the island of Curacao by Werbata in 1908. Map B is taken from DeBuissonje and Zonneveld (1976) (original air photo taken during an undocumented survey in the 1960's). Map C is a 1989 air photo

from KLM AeroCarto survey and Map D is a 1998 air photo from the Curacao – DOW survey.

Close inspection of these maps shows that the rate of mass wasting along the cliff face over the past century has not been significant in the period of 1906 to 1998. However, the presence of the fissures at the top of the cliff indicate the possibility that sudden mass wasting events could occur that are triggered by earthquakes or heavy rainfall events.

**v. Geologic structure of Caracas Bay Peninsula.** In this area that forms the eastern edge of Caracas Bay, the geology is quite different from Seroe Mansinga probably as a result of the more extensive sliding of limestone along its contact with basalt (Fig. 1). The basal basalt is much more extensively exposed as are large boulders of the Seroe Domi Formation that range in size from car to house size and sit directly on basalt (Figs. 1, 5). Based on the low-angle contacts between basalt and the limestone blocks, we assume a low seaward dip of the basalt (~10 degrees) as inferred beneath Seroe Mansinga (Fig. 1). The area near Fort Beekenburg exhibits variable dip directions. We interpret this as a large semi-coherent limestone block that has partially slid along the basaltic contact.

**vi. Geological Controls on Slide Timing: the Holocene notch.** Sea-level studies have shown that approximately 6000 years ago, Global sea level was between 2 and 4 meters higher than what we observe today. Evidence for the 6000 year old sea level high-stand is sometimes preserved as a horizontal erosional feature in limestone (bio-erosion often occurs where the surf hits the shore) (see Figure 6, 7). The previous sea level high stand can also be determined from the height of coral reef platforms that grew during this period (see Figure 8). This erosional line is often referred to as the “Holocene notch” (See figure 6).



*Figure 6. View of early Holocene notch indicated by yellow arrows about 3 meters above sea level next to pier at east side of Caracas Bay. The notch is carved in a large block that we infer was created during the catastrophic Caracas Bay slide about 14 ka. Eustatic sea level studies indicate that the notch is about 6 ka. The horizontal nature of the notch indicates that the block has not moved over the past 6 ka.*

By noting where this notch does and does not exist along Seroe Mansinga and Caracas Bay, we can estimate what features along the shore line were in place 6000 years ago and what features are younger than 6000 years. The existence of the Holocene notch at shoreline boulders adjacent to Ft. Beekenburg (figure 6, 7) clearly indicates these boulders have been in place for at least 6000 years. These boulders are considered part of the upper-terrace limestone formations on Curacao, and therefore, and are not oriented in their original upright position. They were likely placed in their current position during the major slide event that formed Caracas Bay. The fact that we can trace a Holocene notch across these rocks therefore indicates that the slide that emplaced the rocks occurred at least 6000 years ago.

The Holocene notch was also found along nearly all of the south shore (see figure 9) of the APNA property, indicating that this region has experienced little erosion for at least the past 6000 years. The one region on the property that we could not find a clear Holocene notch, however, was the cliff face along Seroe Mansinga. The fact that the notch exists elsewhere in Caracas Bay, but not at the cliff face gives credence to the idea that one major event formed the bay more than 6000 years ago, but since then, smaller-

scale erosion has occurred along the cliff face. At the very least, the missing Holocene notch indicates the entire length of the cliff face has experienced irregular, but likely ongoing, erosion during the past 6000 years.



*Figure 7. View of early Holocene notch indicated by yellow arrows about 3-4.5 meters above sea level south of Fort Beekenberg on the east side of Caracas Bay. The notch is carved a large block highlighted in the circle that we infer was created during the catastrophic Caracas Bay slide about 14 ka. Eustatic sea level studies indicate that the notch is about 6 ka. The horizontal nature of the notch indicates that the block has not moved over the past 6 ka. The area of the beach club marks the southern extent of the debris field formed by the large limestone blocks. To the left of the area marked Beach Club, limestone blocks can be observed sitting directly on Cretaceous basalt. To the south beneath the hill of the Old Customs House, the rocks consist of Miocene sedimentary rocks dipping 25-28 degrees to the south.*



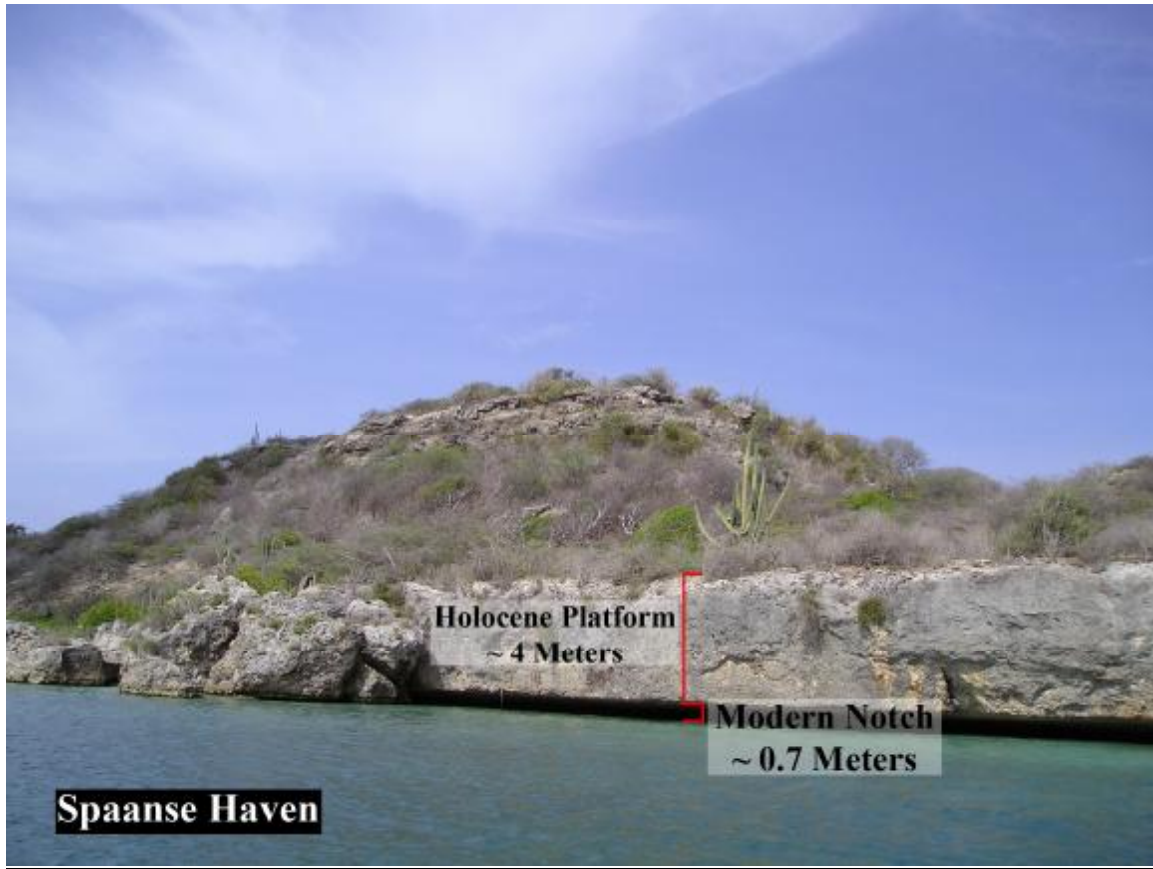


*Figure 8. View of early Holocene platform indicated by red bar about 3-4 meters above sea level on the south side of Spanish Water (Spaanse Haven). Note the presence of the modern sea level notch less than 1 meter above sea level. The top of this platform would correlate with the early Holocene notches shown in Figures A.1 and A.2 and indicates the stability of this area for a period of 6 ka.*



*Figure 9. View of Holocene (6000 year old) notch, approximately 2-4 meters above sealevel, above the current modern notch, along the south side of the APNA property. Evidence for a nearly continuous notch along the south shore indicated that this shore line has remained stable, and that the south shore has not undergone any significant erosion for at least 6000 years. This is not true along the Seroe Mansinga Cliff, where no clear or continuous Holocene notch is observed.*

### **C. Marine Survey Results**

During our week-long study of Caracas Bay and Seroe Mansinga, we collected more than 50 km of high-resolution seismic data across Caracas Bay that includes both the south and eastern flank of the APNA property at Seroe Mansinga (Fig. 10). All of these data have been processed and analyzed. We have merged these data to create high-resolution 3D images of the site, and these images reveal valuable information regarding the size, timing, structure, and number of slides at Caracas Bay and the future stability of Seroe Mansinga.

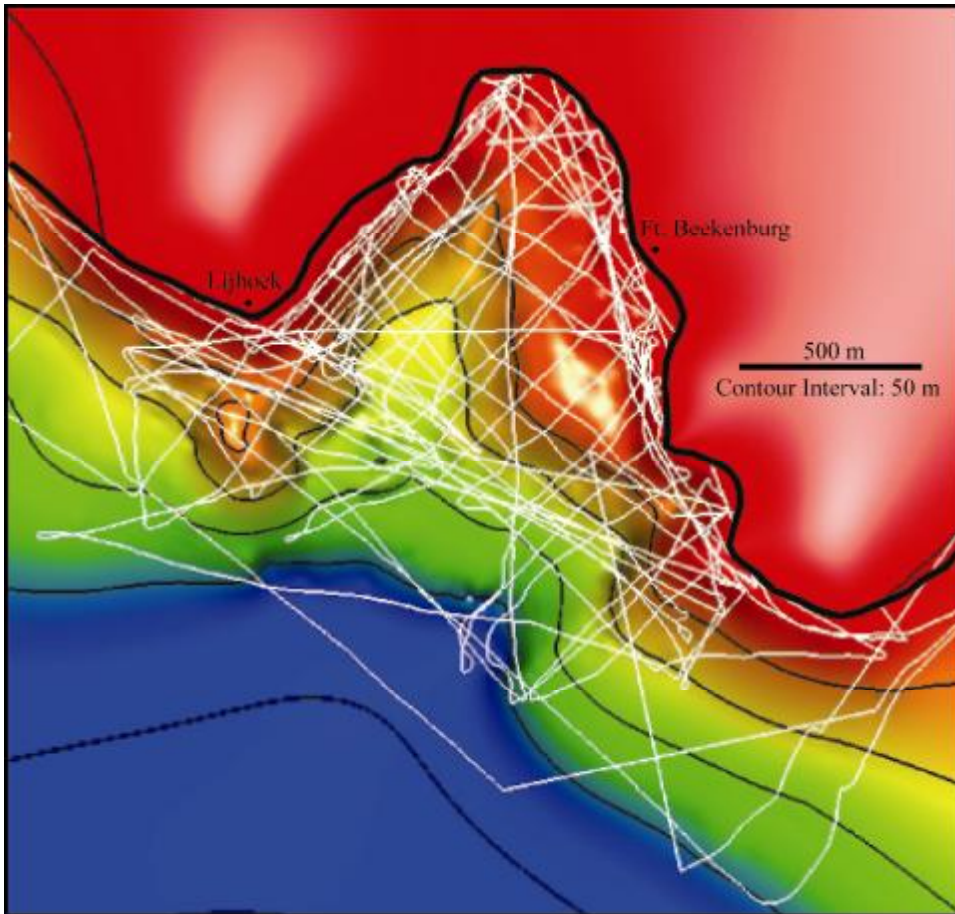


**Figure 10.** Map view showing the location of seismic lines (white) collected in Caracas Bay and along the southern edge of the Seroe Mansinga property. The bathymetry and contours projected on the image were created by merging and interpolating the 2D seismic lines into a 3D image.

**i. General Seismic Observations.** We use the seismic data to create an initial 3D image of the seafloor of Caracas Bay and the seafloor south of Seroe Mansinga. These images reveal a large carbonate reef platform located along the eastern flank of Caracas Bay, as well as a knob-shaped pinnacle reef carbonate platform just southeast of the lighthouse off the southeast corner of Seroe Mansinga (Figs. 11A, B, C). We located one historical map of the Caracas Bay region from the 15<sup>th</sup> century that showed a river system that emptied into the bay from the northwestern corner near the small lagoon. The large eroded channel bed that runs north-south along the western half of the bay is likely the downdip extension of this channel that was infilled to form the causeway connecting the mainland to Caracas Bay Peninsula (Fig. 1). This river channel, which deposited silt and other particulates into the base of the bay indicate why reef formation likely did not occur in this region following the slide. Slide-blocks along with other debris are clearly



imaged at the base of this channel and approximately 500 m southeast of the lighthouse (Fig. 11B, C).

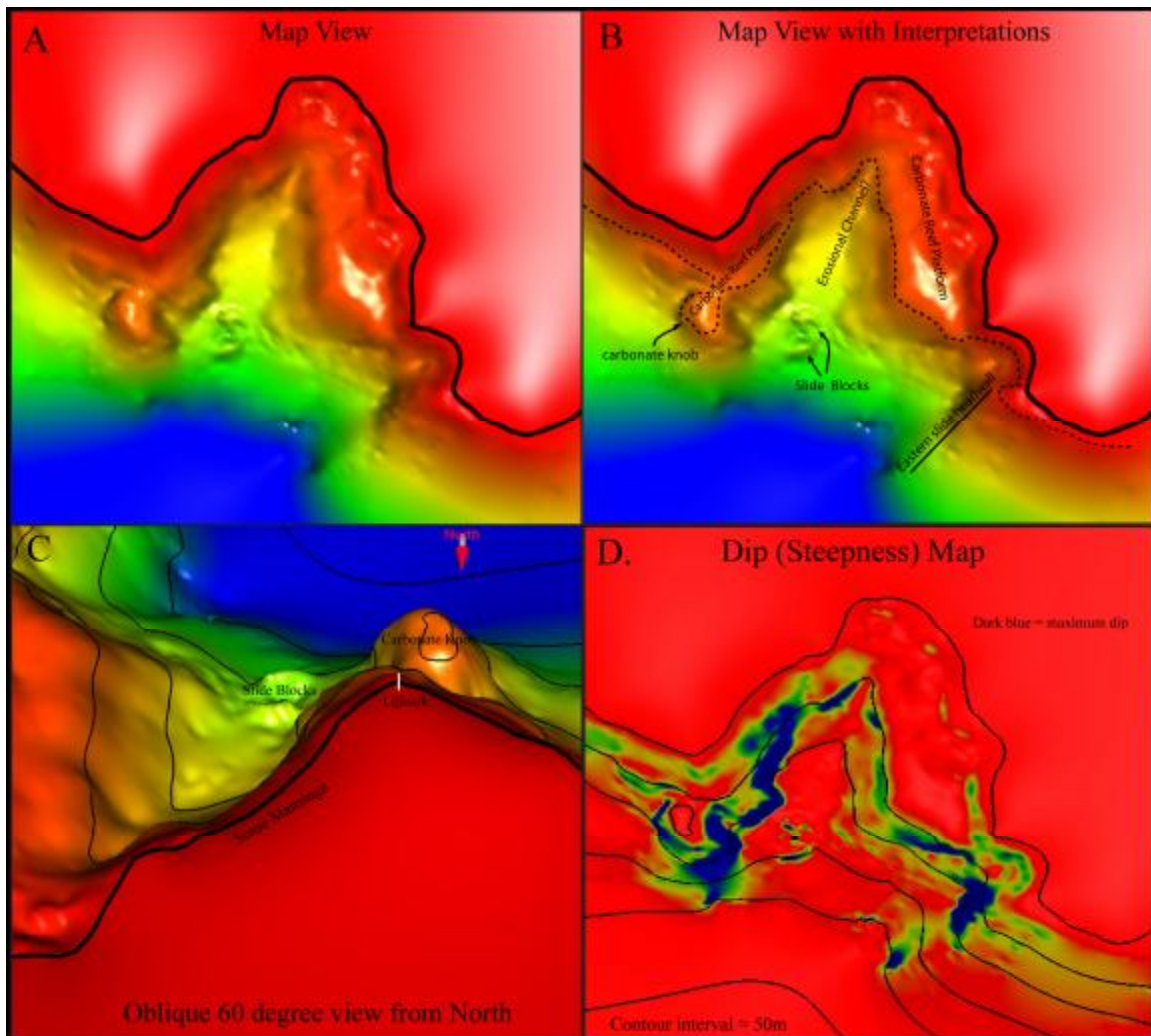


**Figure 11.** Bathymetric and dip (steepness) images of the seafloor with basic geologic interpretations. (A) Uninterpreted image with red representing the land surface and blue representing the deepest water depths. The dark black line is the shoreline. Image (B) is the same as (A) but with basic geological interpretations added. The dashed line in (B) shows the outer edge of the carbonate platform. Note the carbonate platform encircles most of Caracas Bay but narrows along the western headwall adjacent to Seroe Mansinga. (C) Oblique (60 degree) view from the north overlooking the APNA property. No significant reef formation occurs due east of Seroe Mansinga. Contour interval in (C) is 50 m. (D) Location of steepest slopes below sea level (in blue) and flat areas (red) beneath Caracas Bay. Note that only moderate slopes exist along the south and southeast edge of the property; steep slopes in shallow water occur only along the central-western edge of Caracas Bay. This is consistent with the interpretation that the western edge of the basin formed the headwall for the Caracas Bay slide.

Analysis of dip (slope steepness) reveals the steepest sub-sea-level slopes generally occur at 50-90 m depth, and usually along the seaward flanks of carbonate reef platforms (figure 11B, D). Our study shows that the seafloor dip due south of the APNA

property is moderate, and comparable to other ocean-front property on Curacao, and that no evidence for major slide exists along the south-side of the property. We suggest that small-scale erosion, such as rock-slides will be minimal on the south-side of the APNA property since the slope is moderate, and the surface rocks appear both continuous and well-lithified where they dip into the ocean. Furthermore, evidence for a fairly continuous Holocene erosional notch on the south side of the property (discussed earlier) supports the notion that this part of the property has experienced significantly less erosion during the past 6000 years, as compared to the Cliff face. Along the extreme eastern side of the property, however, the slope angle is steep both above and below sea-level, making this area more susceptible to failure. More importantly, the lack of a large carbonate reef shelf along this edge (as compared to the wide carbonate shelf on the eastern side of the bay) or a clear Holocene notch, indicates that large-scale mass-wasting and erosion along the cliff edge has occurred in the recent past. To determine the rate that this cliff is eroding requires constraints on both the age of the slide, and the number of previous slide/erosion events.

## **ii. Constraining Slide Timing, Cliff Erosion Rates, and Frequency with Seismic**

**Data.** We use seismic, coring, and geological data to place improved constraints on slide size and timing. DeBuissonje and Zonnenfeld (1976) suggested that the slide occurred sometime within the last 30,000 year, but, indicate, that the slide may be much younger, and perhaps occurred less than 10,000 years ago. Here, we use seismic data to improve our constraints on slide timing.

In general, directly landward of the steepest submarine slopes are flat carbonate reef platforms which formed after the main slide occurred. As figure 11D illustrates, a maximum dip consistently occurs at ~50-100 m water depth across Caracas Bay. We infer that this consistent slope feature of Caracas Bay is a result of vertical reef building that occurred as Holocene sea level rose over the past several thousand years (Fig. 12).

Specifically, coral reefs only form and grow in a narrow depth range (usually within 50 m) in shallow water, and the observation of a steep slope next to a carbonate platform that has filled in the slide area reveals that:

(1) the reef post-dates (ie. is younger than) the slide and likely began forming directly *AFTER* the last major slide event;

(2) that the slide must have occurred when sealevel was at least ~50-100 m lower, and

(3), because the reef platform is generally continuous everywhere except along the channel and west of the channel (which represents a relatively small area of the survey area), there has not been another major, catastrophic ( $> 0.5 \text{ km}^2$ ) slide event that has occurred at this site since.

Coral reefs have infilled the slide scarp since the last major slide, resulting in slide “healing” as sea-level rose. Areas where the shallow-water reef appears relatively intact indicates little if any ongoing erosion or seafloor disruption, but areas where the reef appears missing are adjacent to steep surface and subsurface cliffs. We suggest limit reef formation has occurred in regions where erosion is ongoing (thereby disrupting the reef building process). The fact that only a small, shallow carbonate reef platform extends directly east of the central Seroe Mansinga cliff further indicates that erosion continues to hinder reef growth at this site. We propose moderately sized blocks (perhaps  $100\text{-}200 \text{ m}^3$ , as seen in the slide block debris in figures 11A, B, C) have periodically broken off the cliff since the original slide occurred.



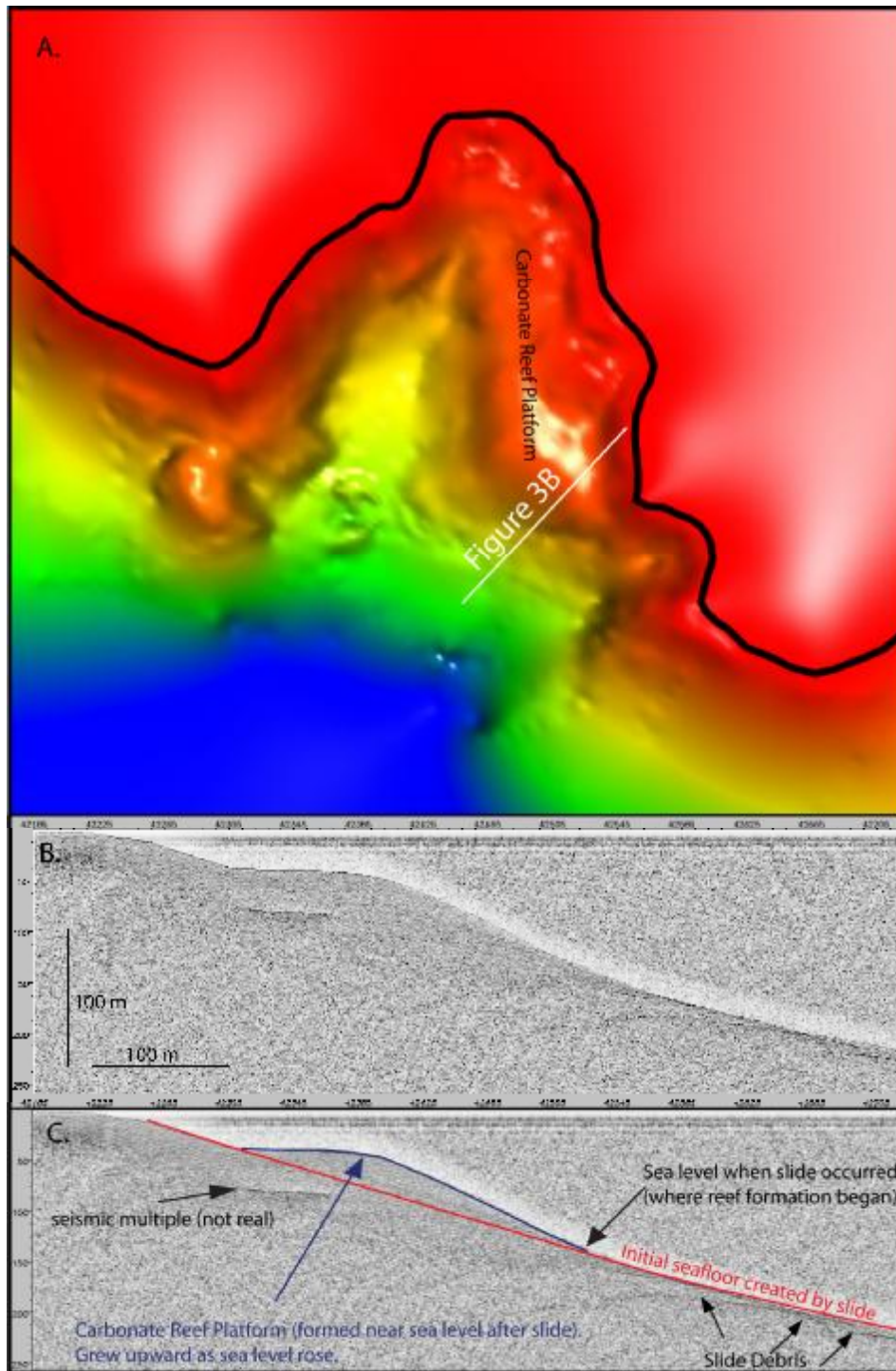


**Figure 12.** (A) Map view of Caracas Bay and the location of the seismic line (white line) shown in Figure 12B and C. (B) Uninterpreted seismic line that starts near the LNG pier at Caracas Bay (left side) and ends ~700 m to the south (right side of line). (C) Geologic interpretation of this seismic line. The red line indicates the original slope of the seafloor, created by the slide, and the purple indicates the location of the carbonate reef. Note that where the carbonate reef ends down slope, slide debris material begins, suggesting that the carbonate reef formation masks the original seafloor structure created by the slide. The carbonate reef platform, however, is significantly smaller in size -or non-existent - along much of the western side of Caracas Bay.

By recognizing that the slide occurred when sea-level was 50-100 m lower (the depth where the reef first began forming), we can estimate the approximate age of the slide event. Previous coral studies (such as Siddall et al., *Nature* 2003) reveal that sea-level has been on average steadily rising over the past 20,000 years. Using modeled sea level curves and seismic data, we estimate that the base of the carbonate platforms (that initially formed immediately following the slide event) are located at water depth of ~50-100m in Caracas Bay (figure 12). From coral dating studies, we know that sea level was 50 m lower ~11,000 years ago, and 100 m lower about ~15,000 years ago. Taking our best estimate that reef formation occurred when sea-level was ~85 m lower, the slide occurred approximately ~14,000 years ago. Therefore, we estimate that the age of the main slide event that formed Caracas Bay is ~14,000 years (+/- 2000 years) (figure 13). As noted above, the carbonate reef platform is relatively intact everywhere, except along parts of the shoreline adjacent to Seroe Mansinga, the western side of Caracas Bay. The lack of a well defined carbonate platform in this location and the evidence from seismic data for slide blocks both below and down slope of this region strongly suggests that ongoing smaller scale mass-wasting has periodically occurred since during the past 14,000 years, after the initial slide occurred (figure 14) .

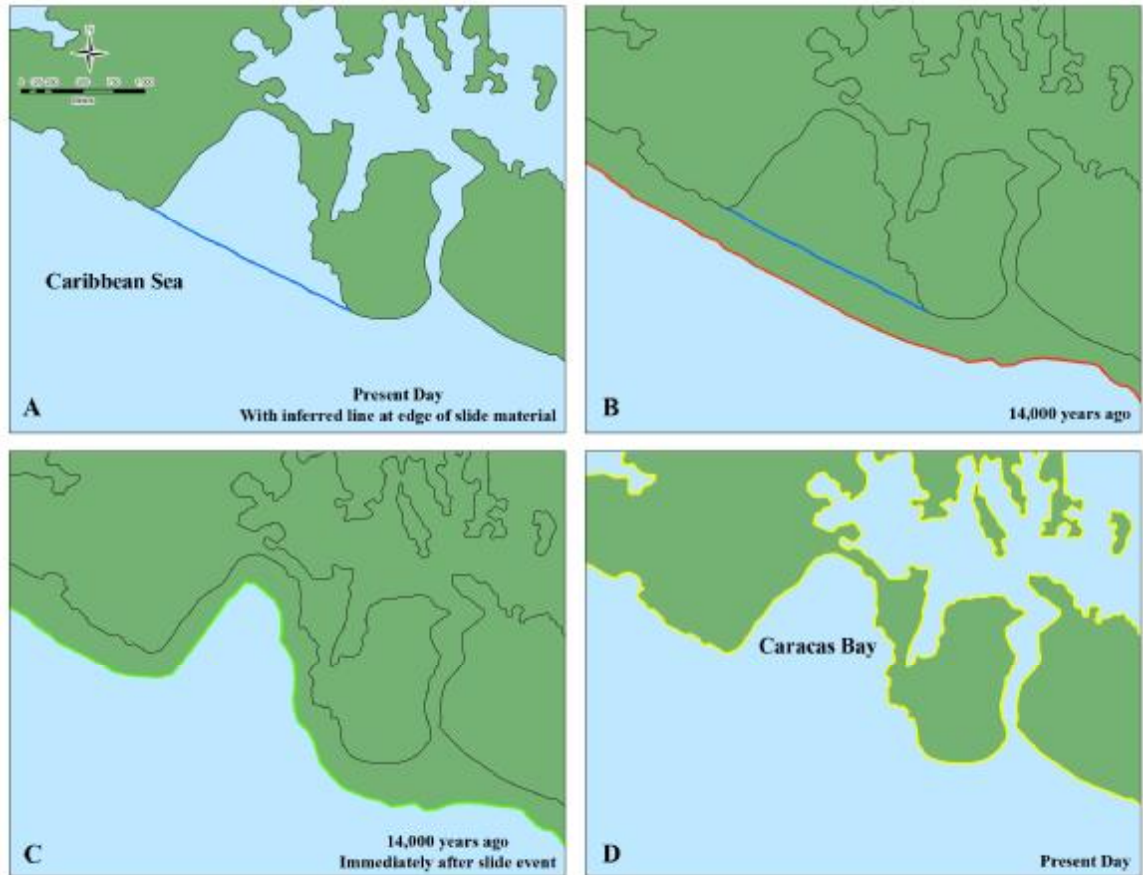


*Figure 13. Cartoon figures showing how the Caracas Bay/Seroe Mansinga Coastline evolved. (A)The southeast coastline of Curacao, near Caracas Bay. The blue line marks the estimated present day coastline across the bay, had the slide not occurred. (B)The red line marks the coastline near Caracas Bay, 14,000 years before present. The coastline is assumed to be fairly straight in front of the area of Caracas Bay because the slide has not yet occurred. The black line marks the present day coastline. (C)The green line marks the coastline of 14,000 years before present, immediately after the slide event. The slide removed large amounts of material, forming Caracas Bay. (D)The yellow line marks the present day coastline in the vicinity of Caracas Bay. The coastline has advanced since the previous image due to sea level rise and erosion along the cliff wall during the past 14,000 years.*

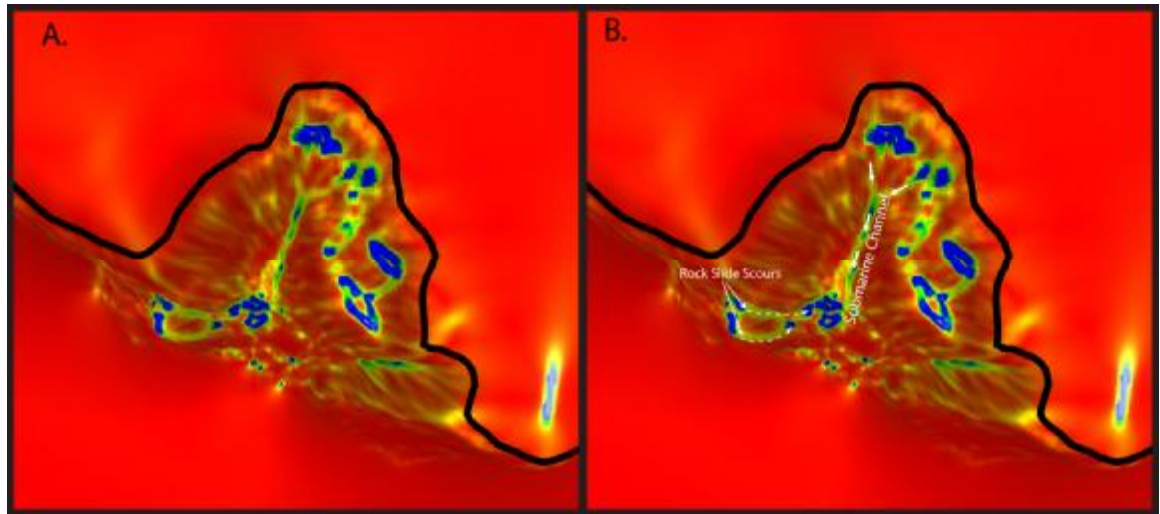


Figure 14. Change in Azimuth-dip angle generated from seismic data, showing the location where concavity/inflection points occur. (A) is uninterpreted, (B) is interpreted. Note the clear evidence for submarine stream bed, which was likely exposed immediately following the slide event, when sea level was much lower. The image also shows some evidence for scour marks from smaller submarine mass-wasting events occurring southeast of the lighthouse. Debris can be seen south of the channel and larger, broader reef-mounds exist in the north and eastern part of the bay.

Again, an independent check on the 14 ka age of the slide is the presence of a Holocene notch at an elevation of about 2-4 meters above sea level. These notches which are known from sea level curves to have formed during a period of elevated early Holocene sea level about 6 ka were observed on a variety of the rock substrates surrounding both Caracas Bay and Spanish Water and include in situ bedrock as well as large limestone blocks that we interpret as slide blocks produced during the slide. The fact that these notches are widespread, occur at the same elevation and affect both the in situ and slumped rocks of the bay suggest that the slump occurred more than 6000 years ago.

The distance from the Seroe Mansinga cliff to the center of the erosional channel (where a thick carbonate platform is lacking) spans a maximum of 350 m (Fig. 1, 12). Using this distance, we estimate a *maximum* average erosion rate of Seroe Mansinga cliff

of 2.5 m/100 years, over the past 14,000 years. The seismic data suggest this erosional channel formed immediately following the slide event, and therefore, it is likely that the cliff did not extend this full distance, and therefore, has eroded perhaps at a lower rate of ~1.5 m/100 years during the past 14,000 years.

Please note, however, that this is an *average* erosion rate, and that this does not mean every 100 years, the cliff will erode ~1 meter. Perhaps more likely is that no significant erosion occurs for 200-500 years (section II and III will discuss timing in greater detail), and then, after a large storm, earthquake, or tsunami, a 5-20 meter section of the cliff calves-off (as evidenced by the size of slide blocks on the seafloor and at the base of the cliff), without further erosion occurring again for another 200-500 years. Indeed, our air-photo analysis (Fig. 3) shows that this may be precisely what happens at least on the time scale of 100 years.

Determining the structural stability of dislodged and overhanging boulders is more difficult to assess than well defined faults, where slip planes, and fault angles are easily identified. Often times, such analysis requires knowing the cohesion of rock varying rock types and the void space below. It has been well documented that storm waves and tsunamis can transport, dislodge, and mobilize meter-scale limestone blocks (for example, see Bryant, 2001). Given the poor cohesion of rocks along the Seroe Mansinga Cliff, it's clear that failures of meter-size boulders will occur every few hundred years when impacted by extreme weather events, tsunamis, or earthquakes. Section 3III will address this issue in greater detail.

### **Summary of Some Key Geological and Seismic Analysis Results:**

- 1. The Caracas Bay largely formed from a single slide event that occurred more than 6000 years ago and likely around ~14,000 years ago.**
- 2. Since the initial slide, most of the region around Caracas Bay and Seroe Mansinga has remained stable, with the exception of the Seroe Mansinga Cliff face, which has been eroding for at least the past 6000 years, at an average rate no greater than 2.5 m/100 years.**
- 3. The south side of APNA property shows no indication of any significant mass wasting or erosion during the past 6000 years.**
- 4. Listric faults exist within the Seroe Mansinga Cliff, but these faults do not clearly outcrop at the surface and have not likely been active in the recent past (last ~14,000 years).**



**Final report: Part II**  
**Analysis of cores from the Caracas Bay region and their implications**  
**for dating the slide and reconstructing historic paleo-storm and tsunami**  
**events**

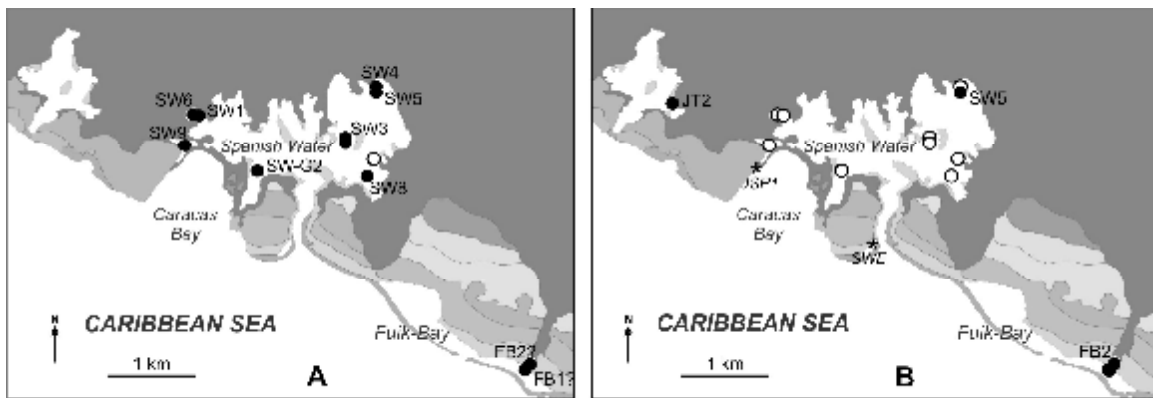
**A. Introduction**

Coastal flooding causing widespread erosion and destruction are primarily the results of extreme ocean waves generated by either tropical cyclones (storms, hurricanes) or tsunamis. The devastating Indian Ocean tsunami and hurricane Katrina events in 2004 and 2005, respectively, dramatically increased public awareness of coastal hazards. Since then government agencies, scientists, and engineers have focused their attention on other regions of the world. The Caribbean is one such region of both, extreme Hurricane risk and tectonic activity, where earthquakes, volcanic eruptions, and submarine landslides are capable of generating tsunami. At least 10 to 12 tropical storms and hurricanes are active each year in the Atlantic Ocean, Caribbean Sea and Gulf of Mexico causing considerable loss of life and property. Tsunamis in the Caribbean have affected more than 22 countries including Central America and northern South America. Thirty-three possible tsunamis are listed for the last hundred years with a major event re-occurrence of about every 21 years. The last destructive tsunami occurred in August 1946 (Lander et al., 2002).

Hurricane and tsunami events inundate low-lying coastal areas with salt water, erode beaches and cliffs, and transport sediments (over wash) inland where they can be preserved as a record of the event. Recent studies reveal that they strongly affect the coastal environment of even remote sites like the Leeward Netherlands Antilles, Southern Caribbean with the Islands of Curacao, Aruba and Bonaire (Scheffers, 2002, 2004; Radtke et al., 2003; Morton et al., 2006). Huge boulder fields and coral rubble ridges are witnesses of paleo-extreme storm and tsunami events; Distinguishing and dating of these coarse clasts deposits in geological records, however, remains a challenge (e.g. Nanayama et al., 2000; Williams and Hall, 2004; Dawson and Stewart, 2007). Following the work of Liu and Fearn (1993, 2000) that successfully identified and dated catastrophic hurricane activities in fine grained lake sediments from coastal inland sites at

the Northern Gulf of Mexico we collected several short sediment cores from the sheltered bays and lagoons near to Caracas Bay. Major goals of this project were the reconstruction and dating of coastal landslide events that potentially could have caused a tsunami wave in the Southern Caribbean and the discrimination and dating of extreme storm and tsunami events that might impact the coastal cliff slope stability in this region.

**Figure 2-1:** Schematic maps of distribution of Hurricane (A) and Tsunami (B) deposit at Caracas Bay. Black full circles show locations with sediment findings. White open circles represent potential findings in deeper sediments.



## B. Coring sites and methods

The field campaign at Caracas Bay in the southeastern part of Curacao Island was carried out in August 2007 and included geological mapping on land, a marine seismic survey and sediment coring in coastal bay and lagoons. Coring locations for marine cores were selected based on high-reflection seismic profile data obtained in Caracas Bay, its adjacent shoreline and Spanish Water Embayment using a high-frequency single channel seismic imaging device. This equipment operates on a CHIRP mode at a main frequency of ~0.5-12 Hz. Navigation aided by GPS resulted in more extensive coverage than previously acquired, providing a vertical resolution of ~10 cm and a penetration of 1-15 m, depending on seafloor geology. Two-way travel times were converted to depth assuming sound traveled through the water column at 1500 m/s. It was possible to recognize changes in sedimentation and structural features within the surface marine sediments. Core locations were chosen based on adequate distances to the open sea (200

– 1500m) such that they could still be influenced by hurricane waves and tsunami events (Fig. 2-1), and on the thickness of soft sediments identified by the seismic data. Cores were retrieved using a 68mm diameter gravity corer.

**Table 2-1:** Coordinates, water depths and core details of samples retrieved from Spanish Water Bay, Fuik Bay and Lagoon Jan Thiel.

Location	Coordinates	Sample	Water depth (m)	Type of sample	Core length (cm)
Spanish Water Bay	N12°04'97" / W68°52'03"	CUR-SW-1	3	core	20
	N12°04'50" / W68°51'51"	CUR-SW-G2a and b	9.3	grab sample	
	N12°04'75" / W68°50'85"	CUR-SW-3-1	11	core	19.5
	N12°04'75" / W68°50'85"	CUR-SW-3-2	11	core	27.5
	N12°05'15" / W68°50'63"	CUR-SW-4	3.5	core	16.8
	N12°05'23" / W68°50'62"	CUR-SW-5	1.5	core	29.5
	N12°04'97" / W68°52'06"	CUR-SW-6	1.5	core	54.5
	N12°04'97" / W68°52'06"	CUR-SW-G6	1.5	grab sample	
	N12°04'41" / W68°50'61"	CUR-SW-G7a and b	5	grab sample	
	N12°04'43" / W68°50'68"	CUR-SW-8	7	core	13.5
Newly opened marina	N12°04'76" / W68°52'09"	CUR-SW-9	2	core	??
Jellyfish pond	N12°04'75" / W68°52'10"	CUR-SW-G10a and b	0.5	grab sample	
Fuik Bay	N12°02'92" / W68°49'35"	CUR-FB-1	2	core	24.5
	N12°02'92" / W68°49'35"	CUR-FB-2	2	core	27.2
Lagoon Jan Thiel	N12°05'06" / W68°52'82"	CUR-JT1	shore	core	17
	N12°05'06" / W68°52'82"	CUR-JT2	shore	core	22
	N12°05'24" / W68°52'77"	CUR-JT3	shore	core	41

13 short cores (<0.5m) were taken from marine and lacustrine environments of the Spanish Water Bay, Fuik Bay and Lagoon Jan Thiel (Table 2-1). The Spanish Water (Spaanse Water Bay) is a modern embayment inland of Caracas Bay connected by a narrow channel to the open sea and adjacent to Tertiary coral reefs and Cretaceous basalts. At its northwestern part it is divided by a 2m high barrier from Caracas Bay. Approximately three quarters of the Spanish Water bay's coastline is urban, and the western part of the bay is used extensively by yachts as an anchorage. Eight sediment cores and nine grab samples were taken mainly from the central and eastern part of Spanish Water Bay in water depth between 1.5m and 11m (Fig. 2-1). Fuik Bay is a shallow ( $\leq 7.3$ m) open lagoon southeast of Caracas Bay. The western part of the bay is used as a loading terminal by the Curacao Mining Company for shipment of phosphate rock. The entire Bay is sheltered by a 3m high mangrove covered reef barrier to the open sea except of a narrow inlet in the central part. Two sediment cores were retrieved from an inland channel in the remote eastern part of Fuik Bay. The lagoon Jan Thiel northwest

of Caracas Bay is a hyper saline lagoon which developed out of an inland bay similar to Spanish Water Bay. It is disconnected by ca 5m high Quaternary coral reefs from the open sea. Three sediment cores were taken from the dry onshore in the eastern part of the lake.

All sediment cores were sliced into 2 halves; one half was kept to serve as an archive and the other half was sub-sampled for analysis. In order to identify storm and tsunami deposits a detailed macroscopic sediment core description and photo documentation were obtained from the archive core half. These analyses included the determination of colors after Munsell soil color chart, sediment structures (grading, bedding etc.), and type and maximum grain sizes of macro components (fossil and rock fragments).

The magnetic susceptibility of each core was recorded in 0.5 cm increments in order to better identify “unusual” sand layers that may represent storm or Tsunami deposits. Samples for sedimentological and mineralogical analyses were taken every 1 cm for each core. The water and organic matter (L.O.I.) content were determined by drying and combusting samples for 24 hours at 105°C and 3 hours at 550°C, respectively. Smear slides were used to identify components, i.e. microfossils of samples that indicate deposition from an extreme storm or tsunami event.

The grain-size distribution of core JT3 from the lagoon Jan Thiel was determined using a Fritsch A-22 Laser Particle Sizer. Samples were taken every 1 cm, weighed (ca 0.3-0.4g) and dissolved in a 5% solution of sodium hexametaphosphate. Each sample was placed in an ultrasonic bath for 2 minutes to disperse clay material before being sieved with a 300µm sieve. The sample fraction larger than 300µm was dried at a temperature of 60° to remove excess water, weighed, and the maximum particle size was measured. The sample fraction smaller than 300µm was rinsed with de-ionized water and centrifuged for 3 minutes at 3500 rpm in order to remove excess water. The residue was analyzed using the Laser Particle Sizer. The laser diffraction patterns were translated to a grain-size distribution according to the Fraunhofer model (Hess and Gatzemeier, 1991). The >300µm fraction data in combination with the laser diffraction results (2-300µm) were used to calculate the median, sorting and skewness for distinct samples.

To establish dates of deposition, organic matter including peat and plant fibers, as well as coral and shell material, was extracted from core sections that document storm or tsunami events and measured at the UCI Keck Radiocarbon laboratory in Irvine, California. Prior to the AMS  $^{14}\text{C}$  analyses all samples were rinsed in de-ionized water and organic matter in addition was leached in 1N HCL and 1N KOH in accordance to protocol for pre-treating radiocarbon samples. Radiocarbon ages were calibrated using the calibration software Calib 5.0.1 and the calibration data MARINE04 for dates on coral and shell fragments (Hughen et al., 2004) and INTCAL04 for terrestrial plant remains (Reimer et al., 2004). Calibrated age ranges are given with a two-sigma standard deviation.

### **C. Results of coring study**

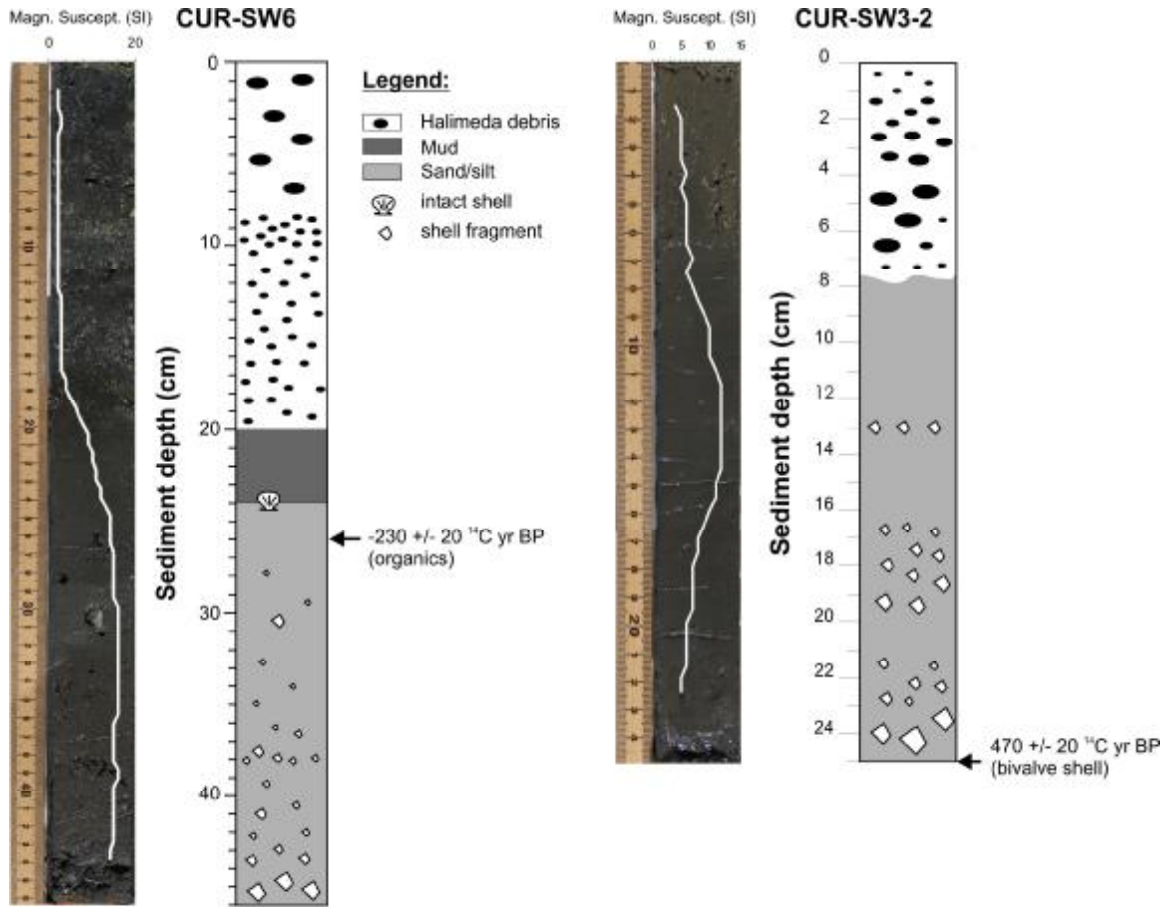
#### **Spanish Water Bay**

##### *Cores SW1 and SW6*

Cores SW1 (16cm) and SW6 (46cm) were both recovered from the western part of the Spanish Water marina at 3m and 1.5m water depth respectively. The banks of this area are heavily built up and several sewer outlets drain into the marina (Fig. 2-1). The topmost sediments of SW1 (5cm) and SW6 (20cm), as well as grab samples SW-G1A and SW-G1B, are dominated by ochre brown *Halimeda* debris (calcareous algae). This is underlain by medium to dark brown coarse sand that fines upwards into silt, which contain abundant bivalve and gastropod intact shells and fragments of *Americardia media* (American Cockle), *Cylichnella bidentata* (Orbigny's Barrel Bubble), *Chione cancellata* (Cross-barred Venus) and *Corbula contracta* (Contracted Corbula). In-situ bivalves of *Heterodonax bimaculatus* (Small false donax) and the Scaphopod *Dentalium antillarum* (Antillean Tusk) were found in the muddy to silty layer at 36-39 cm depth in core SW6. The lower sections of both cores are characterized by a densely packed, very coarse grained shell fragment layer which impeded further penetration of coring equipment. The maximum grain size at the bottom of the cores is 2.5 cm (bivalve shell fragment). The sedimentology of SW1 is similar to SW6, although the sedimentation rates differ due to different water depths and distances to the shore. An increase in magnetic susceptibility is detected at the transition of the normal-graded layer to the

Halimeda debris layer. SW6 radiocarbon dating used organic matter from 26cm sediment depth and indicated a younger than AD1950 deposition of retrieved sediments (Fig. 2-2, Table 2-4).

**Figure 2-2:** Core photos and schematic profiles of cores SW6 and SW3-2 (Spanish Water Bay).



### Grab Samples SW-G2A and SW-G2B

Attempts to core in deeper water in the central western parts of the Spanish Water failed due to lack of fine grained sediments. Two grab samples, SWG2A and SWG2B, were extracted from 9.5m water depth. They consist of a mix of shell fragments and *Halimeda* debris in a coarse sandy matrix.

*Cores SW3-1 and SW3-2*

These cores were extracted at 11m water depth in a channel west of Isla di Yerba, an island in the centre of the eastern Spanish Water. Core SW3-1 is 16cm and SW3-2 is 25cm long (Fig. 2-2). Both cores show similar changes in sedimentation as SW1 and SW6: the upper core sections are dominated by a 7.5 cm thick layer of fine grained *Halimeda* debris, bivalve shell fragments of *Chione cancellata* (cross-barred Venus), Oyster, *Aequipecten acanthodes* (Thistle Scallop) and sea urchin spines. The *Halimeda* debris is finer grained than the *Halimeda* debris of SW1 and SW6. Below this layer is a normal graded sandy to muddy layer containing intact bivalve shells of *Diplodonta punctata* (Common Atlantic Diplodon), *Corbula contracta* (Contracted Corbula), *Arca zebra* (Turkey wing) and worm tube fragments (Table 2-2, Table 2-3). The bottom of the core consists of a coarse grained sand layer. The sediments at the bottom of SW3-2 were found to be modern by radiocarbon dating (Table 2-4).

**Table 2-2:** Distribution of macro fauna in sediment cores from Spanish Water Bay (SW), Fuik Bay (FB) and Lagoon Jan Thiel (JT).

Organism	SW3-2 (11m)	SW5 (1.5m)	SW6 (1.5m)	FB2 (2m)	JT2 (onshore)
Florida Lace Murex		X			
Thistle Scallop	X	X	X		
Cross-barred Venus	X	X	X	X	
Crested Oyster	X	X	X	X	
Contracted Corbula	X	X	X		
Dall's Dwarf Tellin			X	X	
Awl Miniature Cerith				X	
American Cockle			X		
Orbigny's Barrel Bubble			X		
Antillean Tusk			X		
Turkey wing	X				
Small false donax			X		
Common Atlantic Diplodon	X				
Worm tubes	X				
Sea urchin spines	X				
Halimeda	X	X	X	X	X
Crab			X	X	

**Table 2-3:** Details and habitat of macro fauna found in Spanish Water Bay, Fuik Bay and Lagoon Jan Thiel (after Rehder, 1981).



<b>Organism</b>	<b>Organism type</b>	<b>Habitat</b>
Florida Lace Murex ( <i>Chicoreus florifer dilectus</i> )	Gastropod	among coral rubble or in sandy or muddy areas, intertidally to shallow water; North Carolina to southern Florida, and the Gulf Coast to Panama
Thistle Scallop ( <i>Aequipecten acanthodes</i> )	Bivalve	on sand, among turtle grasses, in water 3 - 46 m deep; South Carolina to northern South America
Cross-barred Venus ( <i>Chione cancellata</i> )	Bivalve	in sand, from intertidal zone to water 18m deep; North Carolina to Brazil
Crested Oyster ( <i>Ostrea equestris</i> )	Bivalve	on rocks, from low-tide line to water 107m deep; Maryland to the West Indies
Contracted Corbula ( <i>Corbula contracta</i> )	Bivalve	in sand and mud, in water 3.7 - 28 m deep; Massachusetts, to the West Indies
Dall's Dwarf Tellin ( <i>Tellina sybaritica</i> )	Bivalve	in sand, in water 1.8 - 146m deep; North Carolina to Brazil
Awl Miniature Cerith ( <i>Cerithiopsis emersoni</i> )	Gastropod	on sponges growing on stones, in shallow depths to water 27 m deep; Massachusetts to Brazil
American Cockle ( <i>Americardia media</i> )	Bivalve	in sand, in water 0.3 - 5.5 m deep; North Carolina to Brazil
Orbigny's Barrel Bubble ( <i>Cylichnella bidentata</i> )	Gastropod	in sand, in water 1.8 - 620 m deep; North Carolina to Brazil
Antillean Tusk ( <i>Dentalium antillarum</i> )	Scaphopod	in sand, in water 3 - 61m deep; Southern Florida to the West Indies
Turkey wing ( <i>Arca zebra</i> )	Bivalve	attached to coral rocks and in crevices, from low-tide line to water 6.1 m deep; North Carolina to Bermuda and Brazil
Small false donax ( <i>Heterodonax bimaculatus</i> )	Bivalve	in sand and surf zone; southern half of Florida to the West Indies
Common Atlantic Diplodon ( <i>Diplodonta punctata</i> )	Bivalve	in sand, in water 1.8 - 229 m deep; North Carolina to Brazil
Worm tubes ( <i>Petalococonchus varians</i> )		on solid substrate, intertidally to water 4.6 m deep; Florida to Brazil
Sea urchin spines	Echinoids	intertidal zone to depths of more than 5000 meters
Halimeda	Green macro algae	Lee side of outer shield reefs where flow of nutrient-rich water from the open sea allows them to flourish

**Table 2-4:** AMS  $^{14}\text{C}$  results of samples from Spanish Water, Fuik-Bay and Jan Thiel sediments. \*Calculated reservoir age is 790 years for the Fuik-Bay. \*\*Estimated reservoir age for Spanish water Bay is ca 680 years. \*\*\* Age calibrated using the MARINE04 calibration curve (Hughen et al., 2004).

UCIAMS Lab code	Core, depth	Material dated	$\delta^{13}\text{C}$	AMS $^{14}\text{C}$	2s age range (cal yr BP)
<u>Spanish Water Bay:</u>					
40535	CUR-SW3-2, 25cm	bivalve shell	2.1	470 ± 20**	Out of range
42532	CUR-SW5, 13-14cm	Organic matter	27.0	315 ± 20	456 – 306
40534	CUR-SW5, 13-14cm	bivalve shell	1.2	995 ± 20**	456 – 306
40324	CUR-SW5, 19cm	organics	27.3	1,020 ± 20	963 – 920
40325	CUR-SW6, 25-27cm	organics	25.7	-230 ± 20	< AD1950
<u>Fuik Bay:</u>					
40323	CUR-FB2, 21cm	organics	N/A	365 ± 25	499 – 318
40533	CUR-FB2, 23cm	bivalve shell	1.0	1225 ± 20*	520 – 479
42531	CUR-FB2, 22-23cm	Organic matter	N/A	435 ± 20	520 – 479
<u>Lagoon Jan Thiel:</u>					
40532	CUR-JT2, 17cm	coral	0.0	17,115 ± 40	20,043 – 19,603
40542	CUR-JT2, 19cm	snail shell	-1.3	2,875 ± 15	3,068 – 2,952
42530	CUR-JT2, 19-20cm	Peat	N/A	675 ± 20	673 – 564
40326	CUR-JT3, 15-16cm	peat	22.2	125 ± 20	269 – 0
40327	CUR-JT3, 28-29cm	peat	25.4	135 ± 20	274 – 0
40328	CUR-JT3, 36-37cm	peat	27.4	170 ± 20	285 – 0
<u>Caracas Bay:</u>					
40536	CUR-JSP1	coral	0.0	685 ± 15***	400 – 278
40537	CUR-JSP2	worm tube	-3.5	-505 ± 20	< AD1950
40538	CUR-SWE	coral	-1.1	350 ± 15***	Out of range

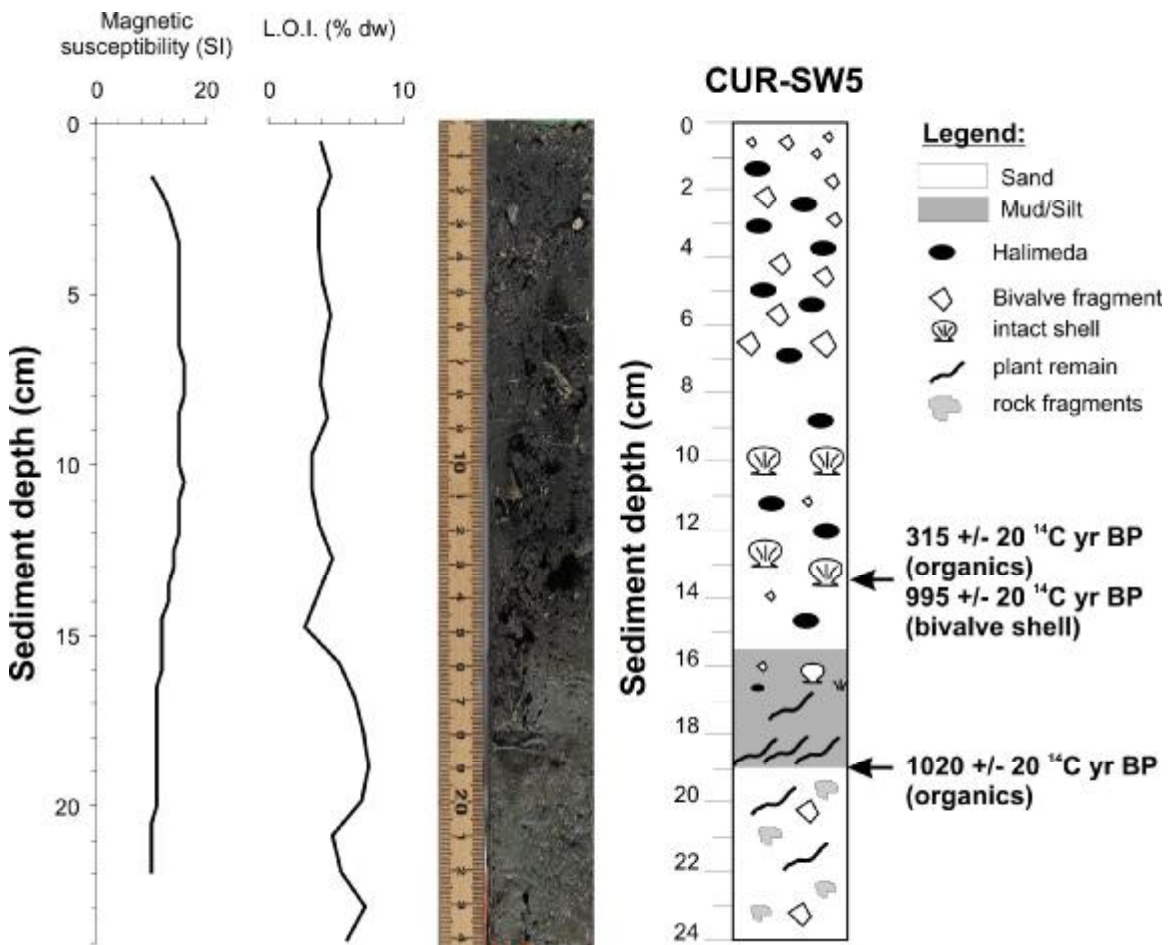
#### *Core SW4 and Grab Samples G4A and G4B*

The base of core SW4 is a medium to dark brownish coarse sand layer that fines upward into silt, which goes up to 5cm. Upwards of 5cm is a sandier layer containing *Halimeda* debris and small shell fragments (<4mm). The bottom of the core contains larger shell fragments (<10mm). The grab samples G4A and G4B match the composition of the top of core SW4.

#### *Core SW5*

This 25cm long core taken proximal to core SW4 at a water depth of 1.5m can be subdivided into 2 units (Fig. 2-3): The topmost 6cm unit contains *Halimeda* debris, smaller shell fragments and sand that fines upwards into silt, similar to SW4. From 6cm to 15cm, the poorly sorted dark brown sediment contains a chaotic mix of large intact older reef bivalves of *Chicoreus florifer dilectus* (Lace Murex,  $\leq 4$ cm) and *Ostrea equestris* (Crested

**Figure 2-3:** Core photos and schematic profiles of core SW5 (Spanish Water Bay).



Oyster,  $\leq 3.5$ cm) and modern bivalve shell fragments of *Corbula contracta*, *Aequipecten acanthodes* (Thistle Scallop) and *Chione cancellata* (Cross-barred Venus). Basaltic rock fragments up to 2 cm in diameter are abundant in the lower 13 cm part of the sediment core. A dark brown muddy, organic rich layer occurs between 15 and 16cm. A visible color change at 16cm marks the boundary between this dark brown layer and the underlying lighter brown sand layer (16-24.5cm). The top of this light brown layer contains shell fragments ( $< 0.8$ mm), whereas the underlying section is dominated by the sand, up to 3cm large basaltic and limestone rock fragments and plant fibers of terrestrial origin. Microfossils observed in thin section include foraminifera (Globorotalia). Two radiocarbon dates on terrestrial plant remains from 13.5cm and 19cm core depth revealed ages at  $315 \pm 20$   $^{14}\text{C}$  yr BP (456 – 306 cal yr BP) and  $1020 \pm 20$   $^{14}\text{C}$  yr BP (963 – 920 cal yr BP) (see Table 2-4). A reservoir effect for the Spanish Water Bay area of ca 680 years has been estimated on the basis of an additional date on marine bivalve shell fragments sampled from 13.5cm core depth.

#### *Grab Samples SW-G7A and SW-G7B*

Extracted from the eastern part of the Spanish Water, SW-G7A and SW-G7B are samples of coarse grained sand containing of fine shell fragments ( $< 5$ mm), rock ( $< 3$ mm) and ostracods. The location was dominated by mangroves.

#### *Core SW8*

This 11.5cm core was extracted from 7m water depth at a location close to grab samples SW-G7A and SW-G7B in the southeastern part of the Spanish Water. The upper 9.5cm is a succession of slightly laminated dark brown mud/silt and coarse sand layers. A coarse grained sandy layer containing bivalve shell fragments is occurring in the lower part of the core. The bottom of the core contains larger shell fragments ( $< 10$ mm). The core composition was similar to the grab samples SW-G7A and SW-G7B and included shell fragments, ostracods and rock fragments. Due to the lack of organic material no AMS  $^{14}\text{C}$  date has been obtained from this core.

#### *Core SW9*

The 12cm long light brownish core SW9 is recovered from a newly opened marina at the northwestern part of Spanish Water Bay. The core is characterized by a 1cm fine sand layer at the top of the deposit and underlain by 11 cm thick mixed gravel layer of Halimeda debris, limestone rock fragments, foraminifera, plant remains and large bivalve fragments at the bottom of the sediment core. This deposit might derive from a wash-in event related to strong rainfall or storm activities.

#### *Grab Samples SW-G10A and SW-G10B*

These grab samples were taken from a jellyfish-infested pond at the foot of a cliff on the western edge of Caracas Bay. They contain limestone rock fragments, plant matter, algae, pelagic foraminifera (*Globorotalia*) and gastropods.

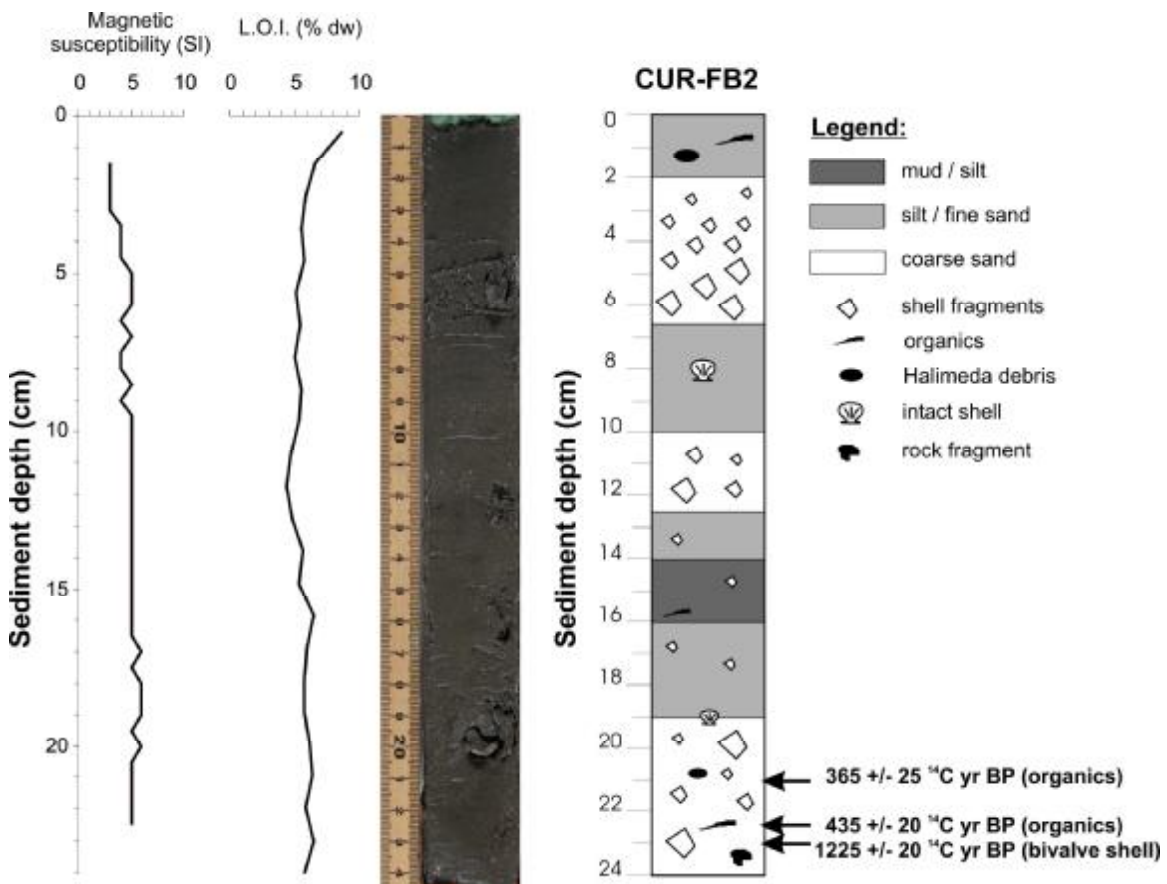
### **Fuik Bay**

#### *Cores FB1 and FB2*

Two sediment cores 20cm and 24cm long were recovered from the southeastern inlet channel of Fuik Bay. The water depth was 2m. The coring site was surrounded by mangroves. The cores are identical in their lithology. Both are slightly laminated and normal graded, with coarse sand at the bottom fining upwards into silt. Core FB2 contains three sandy layers of bivalve and gastropod shell fragments, minor terrestrial organic matter and Halimeda fragments in 2-6.5cm, 10-12.5cm and 19-24cm depth (Fig. 2-4). Scattered large broken and rarely intact shells of *Chione cancellata* (Cross-barred Venus), *Tellina sybaritica* (Dall's Dwarf Tellin), *Cerithiopsis emersoni* (Awl Miniature Cerith) and older reef Oyster shells occur in all of these layers (Table 2-2, Table 2-3). Basaltic rock fragments and plant remains are concentrated in the lower section of the core. Microscope analysis showed many marine microfossils like marine gastropods and foraminifera (*Globorotalia*) throughout the core. Three ages from a bivalve shell of *Tellina sybaritica* from 23cm core depth and terrestrial organic matter from 21cm and 22.5cm depth reveal ages of  $1225 \pm 20$  <sup>14</sup>C yr BP,  $365 \pm 25$  <sup>14</sup>C yr BP and  $435 \pm 20$  <sup>14</sup>C yr BP, respectively (Table 2-4). Calibration of ages of terrestrial plants indicates a

deposition during the last 500 cal yrs BP. Accordingly, a reservoir age of ca. 790 years could be estimated for the Fuik Bay ocean water.

**Figure 2-4:** Core photos and schematic profiles of core FB2 (Fuik Bay).



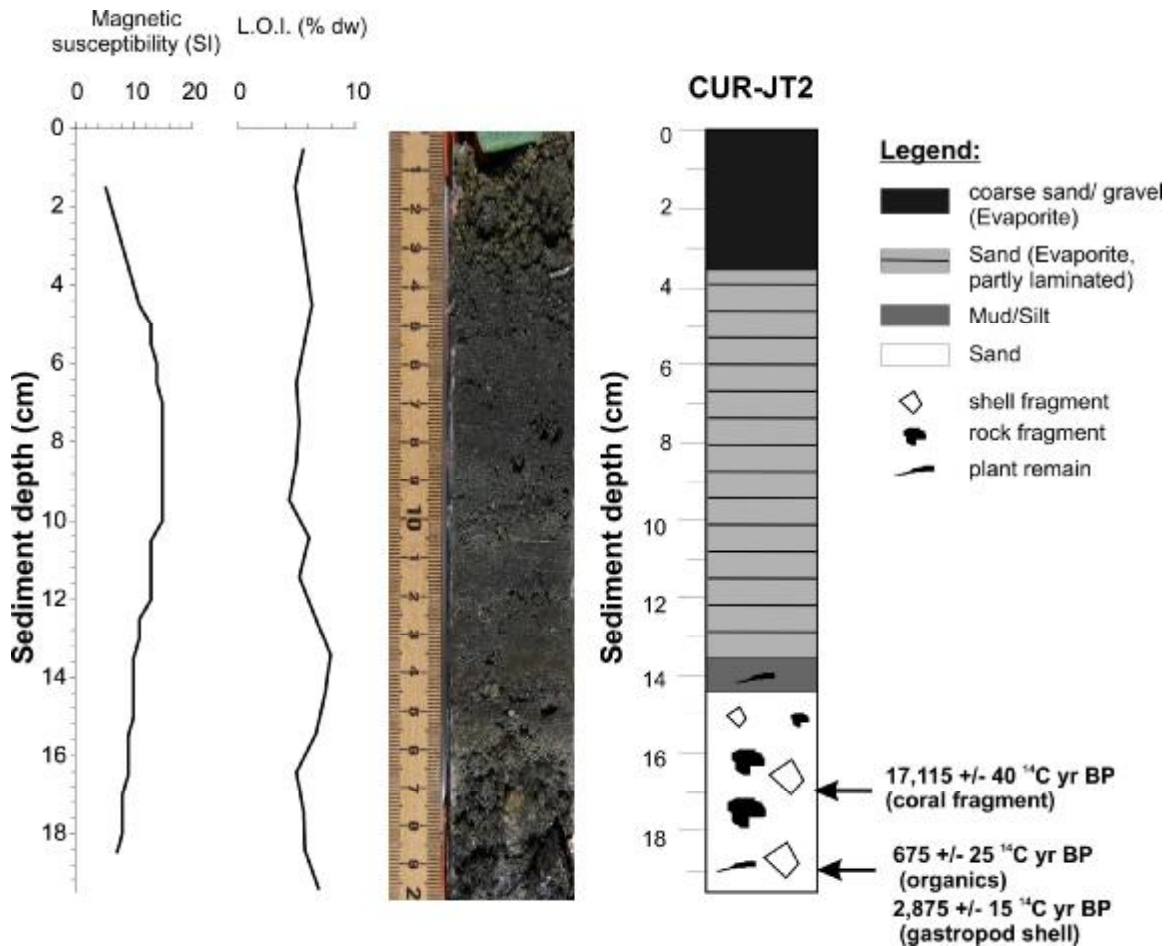


## Lagoon Jan Thiel

### *Cores JT1 and JT2*

Both cores, 16cm long respectively, are from the same location in the central-eastern shore of Lagoon Jan Thiel (Fig. 2-1). They are intensely laminated, with many laminae averaging 2mm in thickness and involve changing grain sizes. The cores contain evaporates (halite and gypsum) of varying grain sizes. A 2cm-thick layer of halite tops both cores (Fig. 2-5). The bottom of JT2 (15-20cm depth) contains a gravelly layer consisting of basaltic rock fragments, *Halimeda* calcareous algae fragments, coral fragments, bivalve, oyster and gastropod shell fragments (up to 32 mm). The larger shell

**Figure 2-5:** Core photo and schematic profiles of core JT2 (Lagoon Jan Thiel).

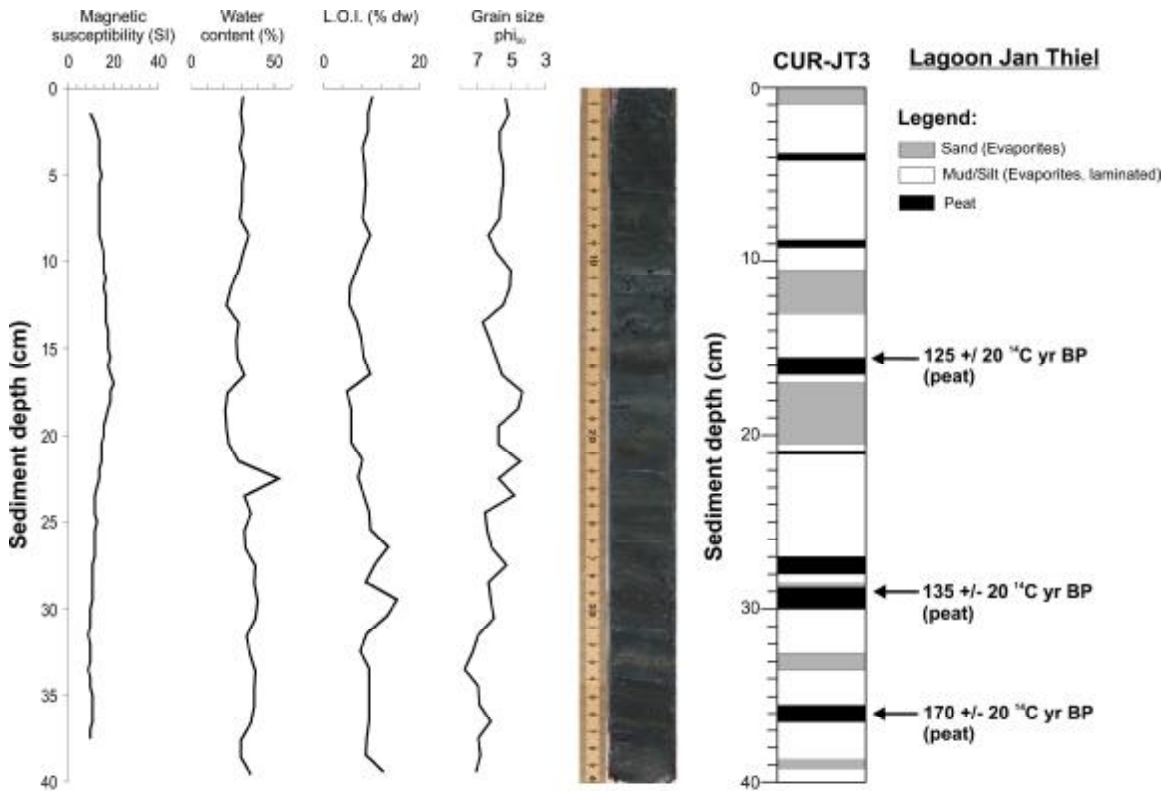


and coral fragments (up to 3cm) are suspected to be from older Holocene reefs. Basaltic rock and limestone are also present along with abundant organic material. The gravel layer is overlain by an organic rich mud layer. Radiocarbon dates were obtained from a coral fragment (17cm) and a snail shell (19cm) and revealed AMS dates of ca. 20,000 and 3,000 years respectively (Table 2-4). The dating of organics from 19.5cm depth reveals an age at  $625 \pm 20$   $^{14}\text{C}$  yr BP (673 - 564 cal yr BP). A reservoir effect for Laguna Jan Thiel is not known yet; therefore ages from shell fragments have to be handled with care.

### *Core JT3*

This core was taken from a more inland location on the southeastern shore of Lagoon Jan Thiel (Fig. 2-1). The 40cm core is intensely laminated and has the same composition as JT1 and JT2 (Fig. 2-6). It is mainly composed of evaporates of varying grain sizes and is intercalated by several peat layers. The evaporite layers represent drier conditions while the peat layers indicate freshwater input. There was no substantial evidence to suggest tsunami or hurricane events in this location. No distinguishable microfossils were seen in thin section. Three AMS dates on peat reveal a deposition in recent times (Table 2-4).

**Figure 2-6:** Core photo and schematic profiles of core JT3 (Lagoon Jan Thiel).



### Coral rubble from Caracas Bay

Coral fragments of *Acropora palmata* collected from coral rubble deposit on land at the slope of the southeastern cliff of Caracas Bay (sample JSP1, Fig. 2-1) have been dated by AMS at  $685 \pm 15$   $^{14}\text{C}$  years BP, which corresponds to a calibrated age of 400 – 280 cal yr BP. A date obtained on worm tubes attached to coral rubble from the same location (sample JSP2, Fig. 2-1) gave negative values and therefore, implies an age younger than AD1950. Coral rubble collected on land in a former lagoon basin at a 5 m elevation at Punta Aballero (sample SWE, Fig. 2-1), the northern part of the entrance to Spanish Water Bay, yield an age of  $350 \pm 15$   $^{14}\text{C}$  yr BP. Calibration of this age using the software MARINE04 failed, since the local reservoir age of 375 – 595 yr BP (Radtke et al., 2003) is older than the original AMS date. Dating on coral rubble collected from proposed tsunami deposits at Jan Thiel Bay (north of Caracas Bay) reveal similar ages at

$674 \pm 37$   $^{14}\text{C}$  yr BP and  $464 \pm 32$   $^{14}\text{C}$  yr BP (Radtke et al., 2003). Though the origin of coral rubble from either tsunami or hurricane events is still under discussion, Scheffers and Scheffers (2006) demonstrated that hurricane waves such as those during hurricane “Ivan” in 2004 and hurricane “Lenny” in 1999 are not energetic enough to destroy coral colonies but are able to redeposit already existing coral rubble ridges. Since Caracas Bay is located at the southwestern sheltered site of Curacao, it is most likely that the rubble fields were formed during a tsunami event and re-deposited during an exceptional hurricane event (i.e. Lenny) as indicated by the modern age of worm tubes.

#### **D. Discussion**

Sediment cores retrieved from Spanish Water Bay comprise at maximum the last 100 years except for the inland core SW5 which is dated at ca 1000 cal yr BP. All cores except of SW8 in the southwestern part of the basin exhibit a top layer of calcareous *Halimeda* debris mixed with fine shell fragments. The thicknesses of these layers and grain sizes of fragments decrease from the northwestern to the southern and eastern part of Spanish Water Bay. Core SW8 instead contains a laminated sequence of sand, silt and fine grained shell fragments. The top layers of all Spanish Water Bay cores are directly underlain by a normal graded succession of large bivalve shell fragments. Most of these bivalves identified inhabit both the shallow bay and ocean zone between 1 and 30 m. The bivalves *Ostrea equestris*, *Tellina sybaritica*, *Diplodonta punctata* as well as the gastropod *Cylichnella bidentata* can occur in water depths up to 250m and 600m respectively. *Halimeda* mound, in turn, are normally found on the outer continental shelf in deep waters behind the reef barrier. They form in response to upwelling nutrients sucked inside the reef wall by tidal currents. The absence of living forms in any of the Spanish Water Bay cores (see also Klosowska et al., 2002) leads to the conclusion that the *Halimeda* debris was transported by high-energy waves generated by a storm event from the open Sea into the Bay area. Two dates on cores SW3-2 and SW6 furthermore suggests a deposition of the debris and the shell fragment layers in very recent times and after 1950. Hurricane Lenny that hit the Island of Curacao in 1999 during its track to the East can be considered as one possible source.

The bottom section of core SW5 in addition shows a “chaotic mixed” layer that is dated at 460 - 310 cal yr BP. Evidence of both large terrestrial components (rock fragments and terrestrial plant remains) and marine macrofossils (older reef and modern gastropods and bivalve intact shells and fragments) suggest erosion and transport by a high energetic wave such as a tsunami. The “chaotic mixed” layer is underlain by a soil deposit that reveals older and most likely reworked plant remains (960 - 920 cal yr BP). Sediment cores from Fuik Bay document at least three shell fragment layers that indicate a deposition from storm and/or tsunami events. The oldest and most coarse grained deposit is dated at ca 500 – 320 cal yr ago; it might represent the top of a tsunami deposit. Dating of the younger storm deposits is in progress and will include Pb-210 dating. So far, only speculations can be made whether the younger storm layer correlates with Hurricane Lenny, and whether the underlying deposit correspond to the 1877 Hurricane event.

Results on sediment cores of Lagoon Jan Thiel reveal no evidence for storm deposits. The basal gravel layer in core JT2 is interpreted as an erosional event that was most likely generated ca 670 - 560 cal yr ago. The triggering mechanism is still under discussion. Most components are basaltic and older reef rock fragments as well as plant remains of terrestrial origin that might have been washed into the lake during a heavy rainfall event. The presence of marine shell fragments of different Holocene and Late Pleistocene ages, Halimeda debris and the mud cap on the top of the deposit on the other hand suggest a marine influence and an origin from a high energetic wave (Tsunami).

## **E. Conclusions**

Having these data on hand, the following sedimentological features can be attributed to distal storm and tsunami deposits in Curacao:

Tsunami deposits in general are broad and landward thinning, with grain sizes that can range from mud to boulders. Tsunami deposits tend to exhibit a small number – in the case of Spanish Water Bay and Lagoon Jan Thiel only one – of homogenous layers that can include mud layers and mud clasts. The mud is deposited in between and after a

wave. The homogenous layers can be a mix of gravel, sand and mud and exhibits marine off-shore as well as terrestrial macrofossils and rock fragments.

Hurricane and storm events, on the other hand, exhibit many parallel layers in thick narrow deposits and rarely have mud layers or mud clasts due to the intense energy involved. Most grains are sand sized. Large shell fragments are abundant and might show normal graded structures. Halimeda debris or any other typical off-shore macrofossils are a good indicator for a high-energetic transport by storm waves into shallow bay areas like Spanish Water Bay and Fuik Bay.

The findings at Caracas Bay indicate that the sheltered part of the Island of Curacao was impacted by Hurricanes and Tsunami during historical times. At least two storm events (Hurricanes) with easterly tracks, most likely Hurricane Lenny in 1999 and another Hurricane in 1877, hit the Caracas Bay and surrounding inland bays. A possible Tsunami event occurred between 500 and 280 cal yr ago as implied by three independent AMS  $^{14}\text{C}$  dates on sediment cores from Spanish Water Bay and Fuik Bay and coral rubble from Caracas Bay. Further evidence is needed whether a gravel layer deposit in Lagoon Jan Thiel sediments refers to the same or an older event.

As an important result of sediment dating, we were able to estimate reservoir ages of the Spanish Water Bay and Fuik Bay on the basis of comparison of AMS dates of terrestrial plant remains and marine bivalve shells. These ages yield at 690 and 790 years respectively. For the Lagoon Jan Thiel, a reservoir age of ca 450 years is estimated by results on AMS dates from the nearby St. Michiel Saline Lagoon (Klosowska et al., 2004).

### **Coring Results Summary:**

- 1. From result, which span over 1000 years, evidence exists that major hurricanes (capable of a 3 m surge above sea-level) appear to occur in this region once every 100-300 years.**
- 2. Moderate sized (~3 m) tsunami may impact this region once every 500-1000 years. No mega (>3 m) tsunami has impacted this region in at least 1000 years.**
- 3. Given that no evidence for a massive tsunami or slide deposit exists in the core data, the analysis confirms the formation of Caracas Bay is not an extremely recent occurrence, and that no major sliding has happened at this site in at least 1000 years. This independent result is consistent with other independent findings discussed in the previous section of this report, indicating that the Caracas Bay slide is at least 6000 years old, and perhaps occurred about 14 ka.**



## **Final report: Part III**

### **Structural and Statistical Analysis of Failure at Seroe Mansinga**

#### **Introduction**

As the seismic data, coring, and geologic interpretation indicate, the current configuration of Caracas Bay resulted mainly from a single major submarine slide event between 6,000-15,000 years ago. Because we now have an idea of both the slide geometry, structure, timing, and size, we can reconstruct the approximate forces acting on the slide and on Seroe Mansinga, and from this, estimate the forces required for failure. Specifically, we can use these data to place constraints on the wind, wave, and earthquake-induced forces needed to trigger failure at Seroe Mansinga.

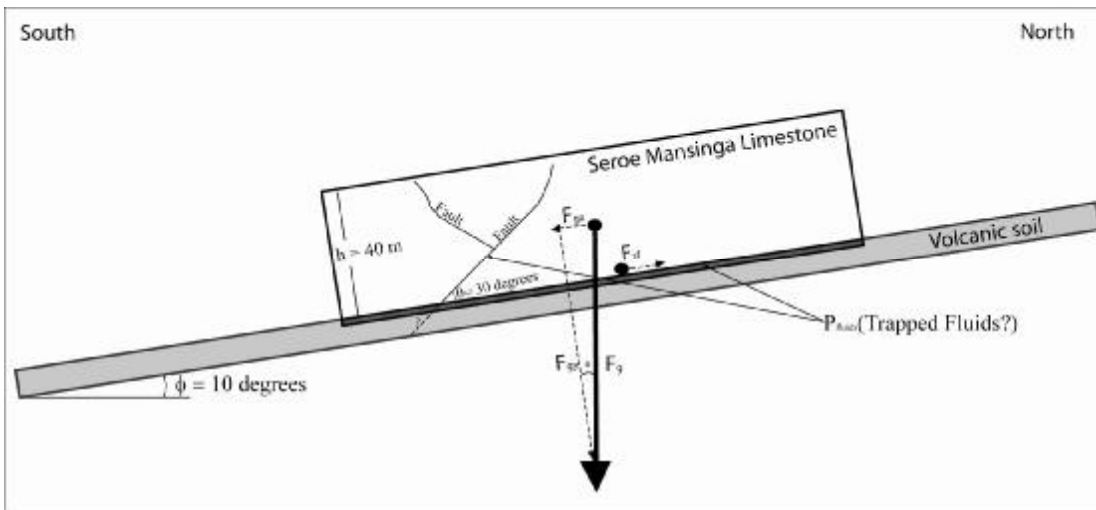
In this section, we begin by generating a simple force diagram from known geological constraints measured on-site. We use these constraints to make end-member estimates for the force required to cause failure at Seroe Mansinga. We first analyze the force required for failure along the limestone-volcanic sediment boundary which dips at ~10 degrees, followed by a failure analysis along previously active listric faults that dip at ~30 degrees within the Seroe Mansinga Cliffs. The analysis is followed by calculations showing the effect wind, waves, earthquakes, and fluid-pressures may have in triggering failure at the APNA property. Our study indicates that relatively infrequent moderate-to-large earthquakes represent the most probable cause of large-scale failure, and that increased sub-surface fluid pressures can significantly reduce the stability at the site. We conclude by recommending an engineering/geotechnical assessment of the subsurface to determine in particular the role of fluid pressures in the region.

#### **I. Failure Analysis Along the Limestone (Seroe Domi)-Volcanic Interface.**

Combining direct measurements at the Seroe Mansinga property and the marine seismic images with measurements by De Buissonje of the Seroe Domi formation in the Caracas Bay region, we estimate that the limestone-volcanic contact along the APNA

property dips seaward an average of ~10 degrees. Given that the this limestone (the Seroe Domi formation) represents an old island-wide slump deposit that broke free from basal rocks during Curacao’s formation (De Buissonje, 1974,1972), we assume that cohesive strength between the limestone and volcanic soil is zero, and therefore, static friction between the limestone unit and the volcanic soil is the key restraining force keeping Seroe Mansinga in place. Furthermore, we estimate a thickness of the Seroe Domi formation at Seroe Mansinga of ~40 m, and a down slope length of ~1 km. Using these values, and assuming an average density of 2000 kg/m<sup>3</sup> for high-porosity fractured limestone, we calculate an average force per unit area (or stress) required to cause failure along the limestone-volcanic soil interface at Seroe Mansinga using the following equations, based on the free-body diagram below (figure 3-1).

**Figure 3-1:** Free-body diagram of the Seroe Mansinga formation on volcanic soil incorporating gravitational, frictional, and possible fluid forces. Buoyant forces are neglected in this scenario.



Force equations for down-slope failure, based on assumptions listed above:

$$F_{\text{failure}} = F_{\text{sf}} - F_{\text{gx}} = \mu (Mg \cos(\phi) - F_{\text{fluid}}) - Mg \sin(\phi) \quad (1)$$

Here,  $F_{\text{failure}}$  is the force required for failure at Seroe Mansinga;  $F_{\text{sf}}$  is the static friction;  $F_{\text{gx}}$  is the gravitational force acting in the down-slope direction;  $\mu$  is the coefficient of static friction,  $M$  is the mass of the failing block,  $g$  is gravitational acceleration,  $\phi$  is the dip of the Seroe Mansinga formation (~10 degrees), and  $F_{\text{fluid}}$  is the fluid pressure at the limestone-volcanic soil interface. To convert this equation from a force equation into a stress equation (or force per unit area, where we no longer need worry about possible slide volume to estimate failure), one must divide both sides by the area of the block in contact with volcanic soil.

Therefore, the critical stress required for failure down-slope at Seroe Mansinga equals the following:

$$S_{\text{failure}} = S_{\text{sf}} - S_{\text{gx}} = \mu (\rho h g \cos(\phi) - P_{\text{fluid}}) - \rho h g \sin(\phi) \quad (2)$$

Where  $S_{\text{failure}}$  is the stress required for failure;  $S_{\text{sf}}$  is the static friction stress;  $S_{\text{gx}}$  is the down-slope gravitational stress,  $\rho$  is the rock density (2000 kg/m<sup>3</sup>),  $h$  is the thickness of the limestone (40 m), and  $P_{\text{fluid}}$  is the fluid pressure.

Before calculating the stress required for failure, it is instructive to note basic conclusions we can draw from 1<sup>st</sup>-order analysis of the above equations. Given that the coefficient of friction is always positive, the reader can see from this expression that:

1. an increase in slope,  $\phi$ , reduces the force required for failure.
2. an increase in the coefficient of friction,  $\mu$ , increases the force required for failure.
3. An increase in fluid pressure,  $P_{\text{fluid}}$ , reduces the force required for failure.

Our greatest unknown is  $P_{\text{fluid}}$  (followed by  $\mu$ , and  $\phi$ ). Calculating this value requires a much more detailed assessment of the limestone-volcanic soil interface, and would likely involve drilling. Nonetheless, we can make some end-member estimates of what this value may be, and use these estimates to place some constraints on failure criteria.

We first calculate the maximum stress required for failure by assuming for now that that  $P_{\text{fluid}}$  is zero, and  $\mu$  is 1. For this instance, the maximum stress required to trigger failure is  $6.36 \times 10^5$  Pa.

Calculating the minimum stress required for failure is more difficult since detailed overpressures measurement are required to know  $P_{\text{fluid}}$ . As a best estimate, we assume that  $P_{\text{fluid}}$  cannot exceed one half the maximum static pressure head generated if an interconnected water-column exists from the highest point on Seroe Mansinga to sea level (approximately 40 meters). Therefore, we estimate a  $P_{\text{fluid}}$  value (equivalent to  $\rho \cdot g \cdot h / 2$ ) of  $3.92 \times 10^5$  Pa. Note: this  $P_{\text{fluid}}$  is an estimate only, and may actually be higher since this is an estimate of the static pore-pressure only. Furthermore,  $P_{\text{fluid}}$  may be higher if (1) fresh ground water can be pumped from below sea-level at or near the site (indicating that over-pressured fluid reservoirs may extend even deeper than sea level) or (2) artesian aquifers are known to exist in the region, or (3) significant ground-water fluid-flow gradients exist (which may results from increased rain or water in-flux). To determine the value of  $P_{\text{fluid}}$  more accurately at Seroe Mansinga requires a geotechnical engineer with pore-pressure analysis experience.

Using our estimated value for  $P_{\text{fluid}}$  and accounting for the possibility that  $\mu$  could be as low as 0.6, we calculate that the minimum amount of stress required for failure along the Limestone-volcanic soil interface is  $2.44 \times 10^5$  Pa. Therefore any stress greater than  $2.44 \times 10^5$  Pa *may* cause failure along this plane, and any stress above  $6.36 \times 10^5$  Pa *will* cause failure.

### **A. The Potential for Hurricanes to Trigger Failure Along the Limestone-Volcanic Interface**

Our analysis of NOAA weather data collected for the past several decades in the tropics indicates that the maximum sustained wind speed every recorded in the southern Caribbean is  $\sim 85$  m/s.

The dynamic stress generated by this wind speed can be approximated using the following wind pressure equation:

$$S_w = \frac{1}{2}(1 + c)\rho_a v^2 \quad (3)$$

Where  $S_w$  is the stress generated along the Seroe Mansinga by the wind,  $\rho_a$  is the density of air (1.29 kg/m<sup>3</sup>),  $c$  is a structural constant that is equal approximately to 1.0 if the wind is striking parallel to the direction of sliding on Seroe Mansinga, and  $v$  is the wind velocity. Using this equation, we calculated that the maximum wind-stress that can be generated on the Seroe Mansinga formation from the strongest wind speeds ever recorded in the region is  $1 \times 10^4$  Pa. As one might expect, this result clearly indicates that even the most severe hurricane winds are an order-of-magnitude too low to trigger failure, and that hurricanes wind alone would have no impact on stability at Seroe Mansinga. The effect of torrential rains, however, by potentially increasing  $P_{\text{fluid}}$  in the region, may have a much more substantial effect in triggering failure. Climate analysis from drilling studies in regions adjacent to Curacao indicate that the climate was significantly wetter ~14,000 year ago when we postulate the Caracas Bay slide occurred (Haug et al., 2001), however, this may simply be a coincidence. Understanding more directly the effects heavy rain may have on regional fluid pressures requires a geotechnical engineering assessment.

## **B. The Tsunami Required to Trigger Failure along the Limestone-volcanic interface**

We can make a first-order calculation of the tsunami wave height required to trigger failure, by using the following hydrodynamic fluid-stress equation (Yeh, 2006) for fluid impacting a structure in quasi-steady-state flow:

$$S_{\text{wave}} = \frac{1}{2} \rho_w C_d h v^2 \quad (4)$$

Where  $S_{\text{wave}}$  is the stress of the wave impacting Seroe Mansinga in the direction of failure,  $\rho_w$  is the density of water ( $1000 \text{ kg/m}^3$ ),  $C$  is the drag coefficient ( $\sim 2.0$  here),  $h$  is the wave height, and  $v$  is the wave flow velocity, estimated to range between 2-5 m/s (Fritz et al., 2006). By setting  $S_{\text{wave}}$  equal to the minimum stress required for failure, we calculate that a tsunami wave between 10 and 60 m high must impact the shore of Seroe Mansinga to trigger failure. It is important to note that a hurricane storm surge, even if it generates floods of this height (which would be a tremendous feat), would likely not have high enough flow velocities to replicate this stress. Thus, hurricane storm surge likely cannot generate enough stress to cause failure in this scenario (assuming again no elevated fluid pressures).

Analysis from a compilation of recorded tsunami wave heights measured for the past 500 years across the Caribbean indicate that wave heights of 10 m have impacted coasts in the Caribbean region four times (O’Laughlin and Lander, 2003). The first wave, estimated at  $\sim 10$  m, came ashore near Salina de Araya and Peninsula de Araya in Venezuela, in 1726. The cause of this tsunami remains unclear. The second wave, which came ashore on November 1<sup>st</sup>, 1755, ranged from 5 to 10 m in height and impacted nearly all of the Leeward and Windward Islands. This wave was generated by the great Lisbon Earthquake of 1755, that occurred directly offshore of Portugal. Importantly, this wave, after refracting and reflecting around the Leeward and Windward Islands lost a significant amount of energy, resulting in only 2-3 meter waves impacting islands to the west. This result nicely illustrates that far-field tsunamis generated by even the largest earthquakes will not likely produce waves big enough to cause failure if they originate outside the Caribbean, since much of the wave energy will dissipate by interacting 1<sup>st</sup> with islands along the Antilles Trench to the north and west of Curacao. The 3<sup>rd</sup> wave, estimated to have a maximum height of 12 to 19 m, occurred in the U.S. Virgin Islands. The Source of this massive wave—the largest ever recorded in the Caribbean—was a Magnitude 7.5 Earthquake that occurred on November 18<sup>th</sup>, 1867, approximately 20 km southwest of St Thomas. The largest waves came ashore in the US Virgin Islands and the Guadeloupe Islands. Further away from the earthquake, the size of the wave decreased, with 1-3 meter waves recorded along the Windward Islands. The fourth and final wave, measured once again as 10 m in height, Impacted Venezuela on October 29<sup>th</sup>, 1900. This

wave was the result of a large earthquake that occurred off the coast of Venezuela, in the region between Isla La Orchila and the Puerto Tuy. This last major tsunami is also the closest event to Curacao (~350 km). Nonetheless, it appears that this wave was local, only impacting the immediate Venezuelan coastline.

Since large ( $> M7.5$ ) earthquakes generate large tsunamis, it is important to assess how often these events occur near Curacao. Historically, none have been recorded. Nonetheless, USGS records indicate that the region has experienced several small-to-moderate earthquakes during the past several decades, and we can use statistical analysis to address the frequency of these and other larger earthquakes. In general, from both regional and global studies of tsunamis, we can say that the generation of a large ( $>10$  m) tsunami wave requires a  $M7.5$  or greater earthquake to occur within 100 km of the impacted shoreline. It has been well documented that earthquakes follow a power-law frequency-size distribution (eg. Gutenberg and Richter, 1954, Malamud and Turcotte, 1999), such that:

$$\text{Log } N = -b m + \alpha \quad (5)$$

Where,  $m$  is the magnitude of the earthquake,  $b$  is universal earthquake constant (the “ $b$ -value”, equal to  $\sim 0.9$ ),  $\alpha$ , a constant, is a measure of the regional intensity or the regional level of seismic activity, and  $N$  is the number of earthquakes in a region per year with a magnitude greater than  $m$ . We can calculate  $\alpha$  directly by recognizing that for the past 35 years (since the USGS kept records of Earthquakes in the Curacao region), there have been a total of 2 earthquakes of magnitude 3.9-4.1 (this magnitude and up is the range where good regional seismic detection exists) within 100 kilometers of Curacao. There has also been a  $M4.8$  (1993, 98 km distant), a  $M4.6$  (1989, 64 km distant) and a  $M4.3$  (1991, 67 km distant). We use the timing and size of these events, along with other smaller events recorded in the region to calculate an  $\alpha$  of  $2.34 \pm 0.3$ . Using the Gutenberg-Richter Law, we therefore calculate that the chance of an earthquake equal to or larger than a magnitude 7.5 occurring within 100 km of Curacao for any given year is 0.004%. To put this number into perspective, the chance of the same size earthquake



occurring in any given year across Southern California is 2.5%, or more than 6000 times more likely. Of course, over time the chance of such an earthquake occurring increases, and using this result, we extrapolate that the probability of a large, magnitude 7.5 earthquake (capable of possibly generating a >10 m tsunami) or greater occurring within 100 km of Curacao during the next 100 years is 0.4%, during the next 500 years is 2%, and during the next 1000 years is 4%. These percentages are likely maximum estimates, since (1) not all large earthquakes will generate large tsunami, and (2) even earthquakes that do generate large tsunami may not have faults oriented in the appropriate position to generate the necessary wave heights at Caracas Bay. Therefore, assuming our estimates for overpressure at Seroe Mansinga formation are reliable, we conclude that the probability of a tsunami triggering structural failure along the limestone-volcanic formation in the next several hundred years is low.

### **C. The Earthquake Required to Trigger Failure Along the Limestone-Volcanic Interface.**

Earthquakes can induce significant ground accelerations in the upper crust of the earth. In general, the larger the earthquake, the larger the maximum ground acceleration produced. Using the force balance equations derived above, and Newton's Second Law of motion ( $F=ma$ ), we calculate that the acceleration required to trigger failure along the Limestone-Volcanic interface (assuming NO fluid pressures at the boundary exist) is 0.79g (where g is the acceleration of gravity). If, however, we assume a 20 m head of fluid pressure potentially exists (as previously described), the acceleration required for failure is only 0.49g. Analysis of acceleration records and statistical analysis of ground acceleration produced by earthquakes indicate that the minimum earthquake required to generate a 0.79g acceleration is a ~M6.2. This event would need to occur within 3 kilometers of Seroe Mansinga. The further away the earthquake, the higher the earthquake magnitude required for failure. For example, an earthquake occurring ~10 kilometers away from Seroe Mansinga would need to have a magnitude of 7.5 or greater to generate the acceleration of 0.79g. As noted previously, the probability of a magnitude 7.5 earthquake occurring within a 100 km radius of Caracas Bay in any given year is

0.004%, and as one might expect, the odds of such an event happening per year within 10 km of Caracas Bay is significantly less (~0.000038%, or once every ~2.5 million years). The probability of a Magnitude 6.2 earthquake occurring within 3 km of the site in any given year is ~0.00005%. Thus, there is only a 0.05% chance of such an earthquake occurring near the Seroe Mansinga region within the next 1000 years.

To trigger failure assuming our low-end acceleration value (0.49g) requires only a M5.3 earthquake to occur within ~3 km of Seroe Mansinga. Using the Gutenberg-Richter Law, Such an event has a 0.0003% chance of occurring every year. This suggests that a 0.3% chance exists that an earthquake may trigger failure of limestone-volcanic contact at Seroe Mansinga during the next 1000 years.

In summary, the probability of wind, waves, and earthquakes generating failure along the limestone-volcanic interface, assuming minimal pore-pressures, is low, with a mega-tsunami and moderate-to-large earthquakes perhaps the most-likely triggers. Furthermore, this analysis only focus on the forces/stresses/accelerations required to cause failure, not continuous sliding into the ocean. The analysis indicates that it is highly unlikely the Seroe Mansinga formation in its entirety will collapse into the ocean within the next several thousand years.

## **II. Analysis of Potential Fault Reactivation within the Seroe Mansinga Limestone Formation**

Because the faults within the Seroe Mansinga formation are situated at much higher angles (the listric faults appear to average ~30 degrees) compared to the low-angle limestone-volcanic interface, the stress required for failure along these faults is lower, and the faults may therefore be more likely to fail than the entire limestone formation. Using equation 2, and assuming the same end-member-estimates for  $\mu$ , we calculate that the maximum stress required for failure along these faults (ie. no fluid pressures) are  $2.87 \times 10^5 - 9.5 \times 10^4$  Pa. *Note that depending on the possible fluid pressure in the fault zone, this value could be much lower, and perhaps close to zero.* Previously, we noted that fluid pressure ( $P_{\text{fluid}}$ ) may be as much as  $3.9 \times 10^5$  Pa depending on subsurface

conditions. If such values existed along these faults as well, failure would instantly occur. Because we don't know the fluid pressures along these faults, we only assess here what *maximum* forces/stress/accelerations are required to cause failure along these faults. *Again, a geotechnical analysis of fluid pressure is needed to know if elevated fluid-pressures exist in this region, and how local watering patterns may charge pore-pressure in these fault zones.*

Assuming no fluid pressures exist along the fault, we again recognize that hurricane force winds are simply too low to cause failure, since maximum stress values remain approximately 1 order of magnitude greater than wind pressures. Analysis of the tsunami wave required for failure (equation 4), however, indicates that perhaps only 4-15 m high wave run-up is needed to trigger fault slip. Approximately 12 tsunamis of this magnitude have occurred in the Caribbean over the past 500 years, although none impacted Curacao (eg. O'Laughlin and Lander, 2003), and the sediment coring study shows no evidence that a mega-tsunami impacted this coast during the past 1000 years. Although it is unlikely that more distant earthquakes can generate these wave run-up values since Caracas Bay is situated on the leeward side of tsunami waves generated by the Antilles and Puerto Rico Trench, earthquakes of magnitude 6.8 or greater occurring 100 km from Curacao may be capable of generating these waves. Using the Gutenberg-Richter Law (equation 5), we estimate the probability of a M6.8 event occurring any given year within 100 km of Curacao at %0.017, or, a 17% chance over 1000 years (~once every 6000 years). Again, the probability of such an event producing a tsunami with the correct orientation and wave height to trigger failure is likely much lower than this.

We can again determine the ground acceleration needed to trigger fault reactivation along the 30 degree faults that dip along the Seroe Mansinga formation using the same Newtonian analysis. From this, we calculate that the acceleration required for failure (assuming no fluid overpressures) is 0.51g, requiring a M5.5 earthquake within ~3 km of the site. The probability of such an event is low (0.2% chance over the next 1000 years. This value changes significantly however, if significant fluid pressures exist along the fault. For example, if fluid pressures are equivalent to 25% of the normal overburden pressure, the acceleration required for failure reduces to only 0.39g, requiring only a

M4.8 for failure. We calculate the probability of a M4.8 occurring within 3 km of Seroe Mansinga on any given year at  $\sim 0.0009\%$ , or  $\sim 1\%$  chance of occurrence every 1000 years. Likewise, if pore-pressure is  $\sim 50\%$  the normal over-burden pressure, acceleration required for failure drops to  $0.26g$ , requiring only a M4.2 earthquake. Accounting for uncertainties, such a small earthquake has between a 3-7% chance of occurring (and therefore, triggering failure) within 3 km of Seroe Mansinga during the next 1000 years. Thus, as this analysis illustrates, the pore-pressure below Seroe Mansinga can significantly influence the stability of the site, and better constraints on fluid pore-pressure will help determine whether failure along these faults is likely to occur on hundred versus thousand-year time-scales. Likewise, fault orientation can impact failure, with steeper faults requiring less for failure. Therefore, if better constraints on these time-scales and estimates are needed by APNA, we strongly recommend they have engineers assess (1) pore-pressures at the property and subsurface structure. It should again be noted that the failure we describe represents only the acceleration/stress for fault initiation and does not necessarily mean these blocks will slide continuously into the ocean. In fact, the offset along the faults in the Seroe Mansinga Cliff indicates that these faults have typically moved only small amounts (less than a few meters) when they were activated in the past. Though we saw no evidence for fluids lubricating or draining from faults along the top or side of the Seroe Mansinga cliff, we were not able to closely analyze all of these faults, (particularly along the cliffs) due to difficulty accessing the cliff-face. Therefore, we cannot rule out the possibility that significant overpressures may exist in this region, nor can we rule out the effects dipping bedding planes may play in focusing fluid flow and generating over-pressures during rainy periods. Furthermore, we cannot address how changing drainage patterns, the emplacement of swimming pools, or lawn watering might impact fluid pressures at Seroe Mansinga, since percolation tests and other engineering-based sediment analysis is required to constrain this. An engineering study that analyzes clay-mixture in the subsurface will also place better constraints on friction coefficients, allowing for more accurate estimates of the failure criteria for a given fault dip-angle. Therefore, to address these questions more thoroughly, we strongly recommend an on-site engineering-based geotechnical analysis.

### **III. A Note on the Impact of Waves, Wind, and Earthquakes on Smaller-Scale Cliff Erosion**

A host of studies (For example, see Bryant, 2001, or Scheffers and Scheffers, 2006) reveal that surprisingly moderate (2-3 m run-up) tsunamis and hurricanes can fracture, dislodge, or move large house-size boulders, similar to those found along and within the Seroe Mansinga Cliff. Our Geological and seismic analysis indicates that large blocks along the cliff have been dislodged and moved perhaps multiple times in the recent past (less than 6000 years ago). Given that both tsunamis and hurricanes can generate waves that trigger these types of failures, and that they happen with greater frequency than large regional earthquakes, we believe that they represent the most likely erosional triggers along the cliff face. Coring analysis combined with NOAA records indicate that large hurricanes or moderate-sized (2-3 m) tsunamis impact the southern coast of Curacao on average every 200-500 years. From these studies, it is clear that the probability for large (several meter diameter) boulders eroding off the Seroe Mansinga cliff every few hundred years is high. The length of cracking along the cliff face combined with the size of some of the largest debris blocks imaged in the seismic data suggests that the eroding blocks may be oddly shaped and as much as 20 m long. This is precisely why we suggested in our initial report that no future development occur within 20 m of the cliff face: the odds of a large (perhaps 5-20 m in length) rock eroding off the cliff over a 200-500 year period is relatively high (particularly since no failure has occurred at this site in the last 100 years). From our seismic study, we suggest that *on average* as much as 2.5 m erodes off the cliff every 100 years. Thus, it should take *on average*, at least 800 years to erode the entire cliff face back 20 m. Ultimately, the decision to build in this region depends on what is deemed risk appropriate by APNA, and whether 100 year time-scales for meter-sized failure along this cliff is acceptable. Given the lack of buttressing along the cliff face and the poorly cohesive nature of the rock and sediments within the cliff, the structural integrity of this region near the cliff is suspect, and we strongly suggest consultation with the appropriate engineers before building anywhere within 20 m of the western cliff face, since failure is likely to occur at irregular intervals in this region over the next few centuries.

## Summary of Structural and Statistical Analysis and Results:

1. **Hurricane winds alone will not generate large scale failure at Seroe Mansinga.**
2. **Assuming only moderate or low fluid-pressures, Significant tsunami waves (at least 4 m high, but perhaps closer to 10 m) are required to trigger fault reactivation or sliding along the limestone-volcanic interface. The probability of an earthquake generating such a wave is low, less than once every 6000 years, and perhaps closer to once every 25,000 years. The probability of this occurring increases if higher pore-pressures or more steeply dipping faults exist.**
3. **It is extremely unlikely that hurricane storm surge will generate failure.**
4. **Assuming moderately low fluid pressures exist along faults, the probability of an earthquake triggering failure along observed faults is very low (less than once every 30,000 years). However, if higher pore pressures exist, faulting may occur more frequently, perhaps on the order of once every few thousand years or less. *Any Increase in pore-pressure or fault angle will further increase this probability, and understanding the impact changing drainage patterns or aquifer recharge in the region has on pore-pressure requires further geotechnical engineering analysis.***
5. **Although this analysis indicates smaller (<M4.2) earthquakes, tsunamis and storm waves would not cause large-scale failure, this does not preclude these events from triggering erosion and smaller-scale instability near (within 20 m) of the more steeply dipping (and more unstable) cliff face. Meter-scale failure in this region will likely continue to occur sporadically every few hundred years.**

### **Recommendations for Future Study:**

- 1. Although we observed no clear evidence for elevated fluid pressures at the site, no direct measurements were made, and we believe it would be valuable to determine directly what (if any) sub-surface fluid pressures exist in the region. We therefore suggest consultation with engineers and an engineering analysis of pore pressure to place more precise constraints on the minimal stresses required for failure at the site.**
- 2. Along similar lines of reasoning, we suggest consulting engineers regarding the effects of changing water drainage patterns (due to construction, watering, well pumping etc.) on fluid pressures, and slope stability.**
- 3. As our results show, the probability of large scale structural failure away from the cliff face is low. This is not true, however, near the cliff. We strongly suggest APNA consult engineers before building within 20 m of the western cliff face, since failure is likely to occur at irregular intervals in this region over the next few hundred years, and building in this region may potentially increase the risk of instability.**



## References

- Beers, C.E., de Freitas, J. and Ketner, P. (1997): Landscape ecological vegetation map of the Island of Curacao, Netherlands Antilles. *Natuurwetenschappelijke Studiekring voor het Caraïbisch Gebied* : 138, Amsterdam, 54 pp.
- Bryant, E., (2001) "Tsunami: the Underrated Hazard," Cambridge University Press, Cambridge, England
- Dawson, A.G. and Stewart, I. (2007): Tsunami deposits in the geological record. *Sedimentary Geology* 200, 166-183.
- De Buissonje, P. H., "Neogene and quaternary geology of Aruba, Curacao, and Bonaire," University of Utrecht Thesis, 1972.
- De Buissonje, P.H. and Zonneveld, J.I.S. (1976): Caracasbaai: A submarine slide of a huge coastal fragment in Curacao. *Nieuwe West-Indische Gid*, Utrecht, pp.55-88.
- Fouke, B.W. (1994): Deposition, diagenesis and dolomitization of Neogene Seroe Domi Formation coral reef limestones on Curacao, Netherlands Antilles. *Natuurwetenschappelijke Studiekring voor het Caraïbisch Gebied* : 133, Amsterdam, 182 pp.
- Fritz H. M., J. C. Borrero, C. E. Synolakis, J. Yoo (2006), 2004 Indian Ocean tsunami flow velocity measurements from survivor videos, *Geophys. Res. Lett.*, 33, L24605
- Fryman, S., Talesnick, M. Geffen, S., and Shvarzman, A., "Landslides and residual strength in marl profiles in Israel," *Engineering Geology*, V. 89. p. 36-46.
- Gutenberg, B., Richter, C.F., "Seismicity of the Earth," Princeton University Press, 1954.
- Haug, G. H., Hughen, K. A., Sigman, D. M., Peterson, L. C., Rohl, U., "Southward Migration of the Intertropical Convergence Zone Through the Holocene," *Science*, vol. 293. p. 1304
- Hess, W.F. and Gatzemeier, M.B. (1991): Vergleichende Untersuchung von ausgewählten Beugungs-Spektrometern. *Chemische Ingenieur Technologie* 63, 378-381.
- Hughen, K.A., Baillie, M.G.L., Bard, E., Bayliss, A., Beck, J.W., Bertrand, C., Blackwell, P.G, Buck, C.E., Burr, G., Cutler, K.B., Damon, P.E., Edwards, R.L., Fairbanks, R.G., Friedrich, M., Guilderson, T.P., Kromer, B., McCormac, F.G., Manning, S., Bronk Ramsey, C., Reimer, P.J., Reimer, R.W., Remmele, S., Southon, J.R., Stuiver, M., Talamo, S., Taylor, F.W., van der Plicht, J. and Weyhenmeyer, C.E. (2004): Marine04 marine radiocarbon age calibration, 0-26 kyr BP. *Radiocarbon* 46, 1059-1086.
- Klosowska, B.B., van Hinte, J.E., Troelstra, S.R. and Laban, C. (2002): Microfacies of Spaanse Water Bay, Curacao (Netherlands Antilles), with special reference to benthic foraminifera. *Journal of Coastal Research* 18 (2), 316-328.
- Klosowska, B.B., Troelstra, S.R., van Hinte, J.E., Beets, D., van der Borg, K. And de Jong, A.F.M. (2004): Late Holocene environmental reconstruction of St. Michiel saline lagoon, Curacao (Dutch Antilles). *Radiocarbon* 46, 765-774.

- Liu, K. and Fearn, M.L. (1993): Lake-sediment record of late Holocene hurricane activities from coastal Alabama. *Geology* 21, 793-796.
- Liu, K. and Fearn, M.L. (2000): Reconstruction of prehistoric landfall frequencies of catastrophic hurricanes in northwestern Florida from lake sediment records. *Quaternary Research* 54, 238-245.
- Malamud, B. D., Turcotte, D. L., “ Self-organized criticality applied to natural hazards,” *Natural Hazards*, vol. 20, p. 93, 1999
- Morton, R.A., Richmond, B.M., Jaffe, B.E. and Gelfenbaum, G. (2006): Reconnaissance investigation of Caribbean extreme wave deposits – preliminary observations, interpretations, and research directions. USGS Open-file report 2006-1293, 41p.
- Nanayama, F., Shigeno, K., Satake, K., Shimokawa, K., Koitabashi, S., Miyasaka, S. and Ishii, M. (2000): Sedimentary differences between the 1993 Hokkaido-nansei-oki tsunami and the 1959 Miyakojima typhoon at Taisei, southwestern Hokkaido, northern Japan. *Sedimentary Geology* 135, 255-264.
- O’ Loughlin, K. F., Lander, J. F., “Caribbean Tsunamis: a 500 year history from 1498-1998,” Kluwer Academic Publishers, Boston. 2003
- Radtke, U., Schellmann, G., Scheffers, A., Kelletat, D., Kromer, B. and Kasper, H.U. (2003): Electron spin resonance and radiocarbon dating of coral deposited by Holocene tsunami events on Curacao, Bonaire and Aruba (Netherlands Antilles). *Quaternary Science Reviews* 22, 1309-1315.
- Rehder, H.A. (1981): The Audubon Society. *Field Guide to North American Seashells*. Alfred A. Knopf, New York, 894 pp.
- Reimer, P.J., Baillie, M.G.L, Bard, E., Bayliss, A., Beck, J.W., Bertrand, C., Blackwell, P.G., Buck, C.E., Burr, G., Cutler, K.B., Damon, P.E., Edwards, R.L., Fairbanks, R.G., Friedrich, M., Guilderson, T.P., Hughen, K.A., Kromer, B., McCormac, F.G., Manning, S., Bronk Ramsey, C., Reimer, R.W., Remmele, S., Southon, J.R., Stuiver, M., Talamo, S., Taylor, F.W., van der Plicht, J. and Weyhenmeyer, C.E. (2004): Intcal04 terrestrial radiocarbon age calibration, 0-26 cal kyr BP. *Radiocarbon* 46, 1029-1058.
- Scheffers, A. (2002): Paleotsunami evidences from boulder deposits on Aruba, Curacao and Bonaire. *Science of Tsunami Hazards* 20, 26-37.
- Scheffers, A. (2004): Tsunami imprints on the Leeward Netherlands Antilles (Aruba, Curacao, Bonaire) and their relation to other coastal problems. *Quaternary International* 120, 163-172.
- Scheffers, A. and Scheffers, S. (2006): Documentation of the impact of Hurricane Ivan on the coastline of Bonaire (Netherlands Antilles). *Journal of Coastal Research* 22(6), 1437-1450.
- Williams, D.M. and Hall, A.M. (2004): Cliff-top megaclast deposits of Ireland, a record of extreme waves in the North Atlantic – storms or tsunamis? *Marine Geology* 206, 101-117.
- Yeh, H., “Maximum fluid forces in the tsunami runup zone,” *Journal of Waterway, Port, Coastal, and Ocean Engineering*, 2006, p. 496